STUDY OF HYDROXYLPROPYL GUAR (HPGG) PROPERTIES AT SOLID-LIQUID INTERFACE

STUDY OF HYDROXYLPROPYL GUAR (HPGG) PROPERTIES AT SOLID-LIQUID INTERFACE

By

ZHEN HU, B.ENG.

A Thesis

Submitted to the School of Graduate Studies

in Partial Fulfillment of the Requirements for

the Master Degree

McMaster University

MASTER (2008) **McMaster University**

(Chemical Engineering) **Hamilton, Ontario**

TITLE: **Study of Hydroxylpropyl Guar (HPGG) Properties at Solid-Liquid Interface**

AUTHOR: **Zhen Hu**

B.Eng. (Tianjin University)

SUPERVISOR: **Professor Robert H. Pelton**

NUMBER OF PAGES: x, 79

Abstract

Hydroxypropyl guar galactomannan (HPGG) properties at solid-liquid interface were studied in this work by investigating adsorption and flocculation behaviors of HPGG with and without borate. Anionic and cationic latex particles were employed to provide the solid-liquid interface.

The adsorption densities of HPGG and HPGG/Borate on anionic latex particles surfaces were determined by the difference of HPGG concentrations in solutions before and after adsorption experiments. The adsorption isotherms of HPGG and HPGG/Borate at different conditions were obtained. Hydrophobic interactions were suggested to be the major source of interactions of adsorbed HPGG and anionic latex. According to dynamic light scattering and electrophoretic mobility data, adsorbed HPGG and HPGG/Borate polymer layer on particle surfaces were discussed.

The flocculation behavior of HPGG, HPGG/Borate, and HPGG/PBA were compared by studying the residual turbidity change of suspensions added with cationic latex particles. Electrophoretic mobility was used as well to study the electrophoretic behaviors of latex particles covered with HPGG or HPGG/Borate. Flocculation mechanisms of this novel flocculation behavior were discussed in this work. With adding more and more monosaccharide into the flocculation, flocs were found to be able to redisperse into the solvent readily. Charge density of HPGG/Borate polymer chain was calculated and the charge density influence on polymer's flocculation behavior was studied.

Acknowledgements

First and foremost I would like to acknowledge my supervisor Dr. Robert Pelton. If it was not his encouragement, trust, guidance and support, I doubt that I would have had the strong motivation and required knowledge to succeed in finishing the project. I am truly grateful to him for giving me the opportunity of studying from him. His inspiring ideas and continuous dedication to solid research will always be what I aim for in the future.

I would like to also thank the past and present members of our research group, Dr. Chengming Li, for giving me some really great suggestions on polymer synthesis, Yuguo Cui, for helping me familiarize myself with this project and teaching me all the basic techniques, Wei Chen and Dan Zhang, for encouraging me when things went wrong in research, and other members in Interfacial Technologies Group, for treating me not only as friends but also family members.

Lastly, I'd like to dedicate this thesis to my family back in China. Their everlasting belief in me has been always keeping me working harder and being better. Their words are always the sweetest things I could ever imagine.

TABLE OF CONTENTS

List of Figures

List of Tables

Chapter 1 Literature Review

Over ten million people in North America suffer from dry eyes. It is usually caused by a chronic lack of sufficient lubrication and moisture in the eye. In dry eye syndrome, the eye doesn't produce enough tears to form the tear film that lubricates the eye, or the tears have a chemical composition that causes them to evaporate too quickly (Christensen, Cohen et al. 2004). When it comes to treating dry eyes, many find relief simply from using artificial tears on a regular basis. Among them, one commercially available product from Alcon is proved to be particularly effective. However, the mechanisms by which this product functions in the tear film and especially the major component hydroxypropyl guar galactomannan (HPGG)'s role in treating dry eye syndrome are still poorly understood. The overall goal of my work is to identify the factors influencing HPGG interactions with surfaces under physiological conditions in the tear film.

1.1 Guar & HPGG

Guar galactomannan, a water-soluble polysaccharide extracted from the seeds of *Cyamopsis tetragonoloba*, consists of a linear backbone of β-1,4 linked mannose main chains to which are attached α-1,6 galactose units, as shown in Figure 1-1. The ratio of mannose to galactose units ranges from 1.6:1 to 1.8:1.

Due to its ability to produce a highly viscous solution even at low concentrations, guar is widely used as a thicker in paper, textile, petroleum-drilling,

pharmaceutics, food and cosmaceutics industries (Cheng, Brown et al. 2002; Srivastava and Kapoor 2005). The high viscosity of guar solutions and a tendency to aggregate during industry processing are caused by the high molecular weight of guar (up to 2 million) and the intermolecular entanglements and physical cross-linking in aqueous solutions through hydrogen bonding. To extend its range of applications in industry, native guar tends to be modified by either chemical or enzymatic methods (Mitchell and Hill 1995). Treatment of guar with ethylene oxide, propylene oxide, and chloroacetic acid in base results in the formation of hydroxyethyl guar, hydroxypropyl guar, and carboxymethyl guar, respectively. However, it is difficult to control the solution viscosity due to microorganism induced degradation which limits its application.

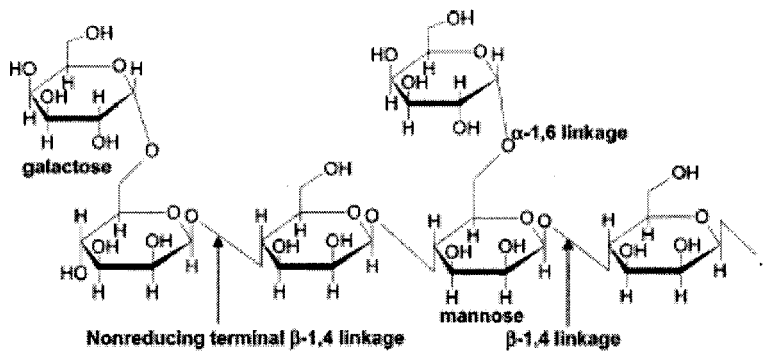

Figure 1-1 The structure of guar galactomannan: guar consists of a linear backbone of β-1,4 linked mannose units and is solubilized by randomly attached α-1,6 linked galactose units as side chains (Mahammad, Comfort et al. 2007).

In many industrial applications, hydroxypropyl guar is the preferred derivative of natural guar because of its better solubility in water compared to unmodified guar.

The extent of hydroxypropyl substitution is usually expressed as a degree of substitution (DS), which is the average number of hydroxypropyl groups substituted per sugar ring. The HPGG used in this work had a DS of 0.36. The intrinsic viscosity and Huggins coefficient for natural guar and HPGG with various degree of substitution at 25 ℃ are listed in Table 1.

Table 1-1 Intrinsic Viscosity, Huggins Coefficient, and Weight Average Molecular Weight for Natural Guar and Various HPGs (Cheng, Brown et al. 2002).

	$[\eta]$, dL/g (25 °C)	k_H (25 °C)	$[\eta]$, dL/g (40 °C)	k_H (40 °C)	M_W
natural Guar	16.39	0.79	16.07	0.73	1.935×10^6
HPG (MS ~ 0.2)	14.65	0.53	15.12	0.43	1.910×10^6
HPG (MS ~ 0.6)	14.51	0.32	14.27	0.29	1.928×10^6
HPG (MS ~ 1.07)	15.43	0.32	14.62	0.36	1.861×10^6
HPG (MS ~ 1.53)	15.92	0.31	14.51	0.37	1.945×10^6

1.2 Borates and Boronates

Sodium borate as common borax ($Na_2B_4O_7 \cdot 10H_2O$) at low concentrations in water dissociates completely to form boric acid, $B(OH)_3$, and monoborate, $B(OH)_4^-$

$$B_4O_7^{2-} + 7H2O \rightarrow 2B(OH)_3 + 2B(OH)_4^-$$

and an acid-base equilibrium is established between these two species

$$B(OH)_3 + H_2O \overset{K_A}{\leftrightarrow} B(OH)_4^- + H^+ \qquad pK_A = 9.0\text{-}9.2$$

The monoborate, $B(OH)_4^-$, binds with *cis*-hydroxyl groups in guar to add a negative charge to the polymer. The consequence of borate binding onto guar is the conversion of nonionic polysaccharide to anionic polysaccharide (HPGG/Borate)

(Pezron, Ricard et al. 1988). Borate can also cross-link molecules because the monoborate anion contains two pair of hydroxyl moieties that can form reversible diester bonds with molecules containing *cis*-diols in a favorable conformation as shown in Figure 1-2 (Sinton 1987; Kesavan and Prudhomme 1992).

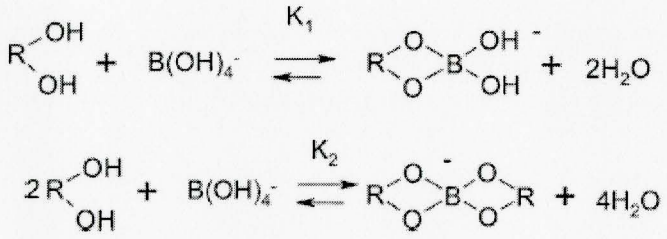

Figure 1-2 Two steps of reaction between borate and polyols.

Addition of borax to guar solutions at alkaline pH gives rise to gels. Carnali claimed that the mechanism involved complexation of the *cis* OH-3 and OH-4 hydroxyl groups on the galactose side unit of guar with boron to induce a five-membered diol ring (Carnali 1992). Complexation of this moiety with a second galactose unite yields a crosslink (Figure 1-3). The nature of these crosslinks is covalent, however, the large negative entropy of formation of the equilibrium constant indicates that they are quite labile with increasing temperature (Pezron, Ricard et al. 1988; Carnali 1992). The lifetime of the guar/borate linkage is estimated in the range of 10-100s. On shorter time scales, the solution behaves as a rubbery network (Saffour, Viallier et al. 2006). In a review by Nijenhuis, the gelation of poly(vinyl alcohol) or PVA by addition of borate ions was discussed. The cross-links of this

polyol-borate complexation are labile as the gels display a liquid-like behaviors at low frequencies and a rubber-like one at high frequencies (Nijenhuis 1997).

Pezron and co-workers studied interactions between borate ion and guar or HPGG. The formation of reversible gel induced by borate complexation was found in their work (Pezron, Ricard et al. 1988). In addition, Prud'homme and his co-workers found the rheological properties of the borate-bound guar gels depend strongly on the number of effective cross-links. Borate-cross-linked guar and HPGG gels change from dilute polymer solutions at high temperatures or low pH values to solid gels at low temperatures or high pH values (Kesavan and Prudhomme 1992).

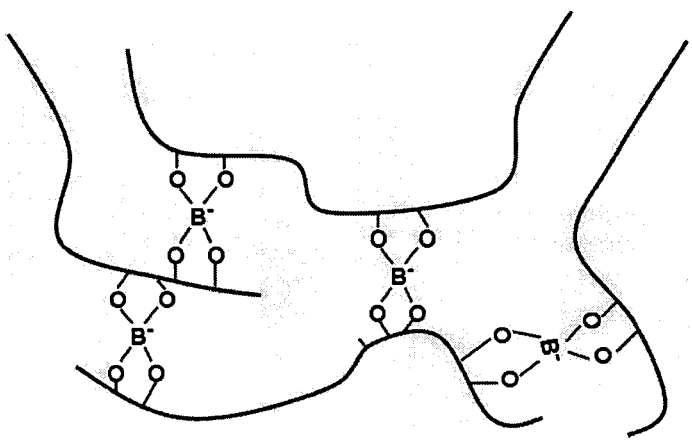

Figure 1-3 Schematic view of a network formed by borate crosslinking of guar.

Through ^{11}B NMR and dialysis experiments, Pezron determined the borate-guar complex structure and the borate binding constant. They claimed that five- and six-membered ring monodiol-borate complexes were formed and complexes were more readily formed on galactose units (Pezron, Ricard et al. 1988). Jasinski and

co-workers, on the other hand, found that the predominant structure is the six-membered ring formed when borate binds with the C4 and C6 hydroxyls on the pendent galactose groups (Jasinski, Redwine et al. 1996). Unlike borate, boronates (i.e. methylboronic acid and phenylboronic acid), however, contain only one pair of hydroxyl moieties and cannot serve to cross-link polyols (Bassil, Hu et al. 2004).

A simple polyelectrolyte can be defined as a homopolymer where the monomer unit carries an ionisable group. The groups may be a strong acid or base, making the polyelectrolyte pH independent. On the other hand, pH dependent polyelectrolyte carries weakly acidic (i.e. carboxylic) or basic (i.e. amino) groups. More complex polyelectrolytes are copolymers where only a fraction of the monomer carry ionisable groups, and polyampholytes which carry both positive and negative charges. Protein for example falls into the category of polyampholytes.

The polyelectrolyte chain is rigid because the internal electrical repulsion is minimal for a straight line configuration. However, the polyol-borate complex ion systems are very different from polyelectrolytes bearing fixed charged groups. The charges on the polyol-borate complex chain are determined by chemical equilibrium between the *cis*-diol and borate ions. There remain some free borate ions present in the solution. These free ions are able to screen the electrostatic interactions of polyol-borate complex chain even in the absence of passive salt. Therefore, the polymer chain conformation of polyol-borate complex is determined not only by the charged units on this polyelectrolyte chain but also by the presence of free borate ions in solution (Chen, Guo et al. 1998; Pelton, Cabane et al. 2007).

1.3. Adsorption

There is a change in composition near the polymer solution/solid interface. And the increase in concentration of the solute in the interfacial region is generally called adsorption. A molecule in solution will adsorb to a surface when the adsorption energy is substantially larger than kT. When it comes to polymer adsorption, even if the energy per monomer contact is relatively small, the number of contacts results in high adsorption energy. Hence, if a polymer has any affinity for a surface, it usually adsorbs strongly and irreversibly. Chain configuration at the surface depends on the balance of entropy- trying to maintain a coil configuration, and polymer/solid interactions which promote a flat configuration (Figure 1-4).

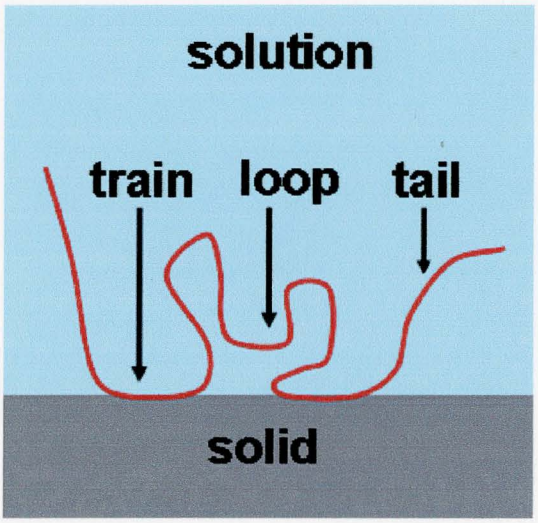

Figure 1-4 Adsorbed polymer configurations at a surface.

Uniform homopolymers show "high affinity" adsorption isotherms in which surfaces are saturated at very low solution concentrations. Polydisperse homopolymer,

on the other hand, gives less ideal isotherm. The nonionic homopolymer that adsorbs from a good solvent onto a surface will not change its coil configuration dramatically. Usually, the thickness of the adsorbed layer is of the same magnitude as the radius of gyration R_g. The chain configuration can be described in terms of tails (the two ends of the chain sticking out from the surface), trains (sequences of the chain that have contacts with the surface), and loops in which the chain makes long extensions into the solution between two trains.

A key parameter for adsorption is the adsorbed amount Γ^{max}. The most widely accepted definition of Γ^{max} is the amount of polymer at the interface in excess of the bulk solution concentration. Adsorbed amounts are normally presented in adsorption isotherm, which is a plot of Γ^{max} as a function of the equilibrium bulk polymer concentration at a given temperature. A typical adsorption isotherm for a monodisperse polymer is shown in Figure 1-5.

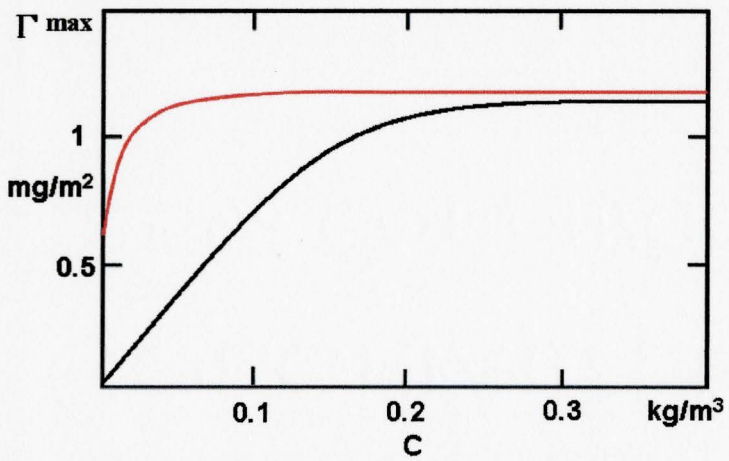

Figure 1-5 A typical high-affinity (red curve) and weak-affinity (black curve) adsorption isotherm: Γ^{max}-adsorbed amount or adsorption density at the interface; C-equilibrium polymer concentration in solution.

As in figure 1-5 a high adsorption density occurs even at extremely low polymer concentrations. For higher concentrations, the adsorption isotherm curve levels off and shows a nearly horizontal part, the plateau, indicating a saturation of the surface. And the plateau adsorbed density normally reaches value of the order of a few mg/m^2.

An adsorption isotherm of this shape is categorized as a high-affinity isotherm. For polydisperse polymers there is usually no such well-defined plateau and a more rounded isotherm occurs.

The adsorption density depends on the competition in interaction between a polymer segment and a solvent molecule with the surface. Therefore, the net adsorption energy depends on the solvent and the nature of the solid surface. With solid substrates strong Van de Waals forces, electrostatic attractions or even hydrogen bondings are possible. However, in some other cases the adsorption is mainly driven by the poor solubility of the polymer and the tendency of polymer sticking to less soluble surfaces. And this force is classified as hydrophobic interaction.

The most widely used methods for obtaining the adsorbed amount and adsorption isotherm are those in which the solid with adsorbed polymer on surface and the solution is separated, after which the supernatant is analyzed (indirect methods). Alternatively, the solid surface is analyzed either in situ or after separation (direct methods). Basically, the indirect method is about measuring the polymer solution concentration difference before and after adsorption. The adsorbed amount can be calculated from

$$\Gamma^{max} = \Delta C_p V/A_s$$

Where ΔC_p is the change of polymer solution concentration, V is the total solution volume and A_s the total surface area. Many techniques like UV, FTIR, and NMR that can determine concentration may be used to analyze the supernatant.

For the direct method, the adsorption density is measured using methods like optical reflectometry, neutron reflectometry, ellisometry, surface plasma resonance, surface-enhanced Raman scattering and the quartz crystal microbalance. Compared to indirect method, the direct method is inherently more accurate because an absolute quatity is measured rather than a difference.

The adsorbed layer thickness is one of the prime factors in determing the effectiveness of an adsorbed polymer layer in stabilizing colloidal dispersions and the microstructure of this adsorbed polymer layer at the surface. A plethora of techniques are currently used to determine the adsorbed polymer layer thickness. They fall into three major categories which are defined as static, hydrodynamic, and disjoining pressure. The static definition involves completely non-invasive techniques that measure various moments of the volume fraction profile, for example by scattering or ellipsometry. The hydrodynamic methods encompasses the measurements in flow; for example flow of solvent through polymer-coated capillaries, quasi-elastic light scattering from diffusing particles or dispersion viscosity measurements. The last category involves the bridging together of two polymer-coated surfaces. As expected, the absolute values of the adsorbed polymer layer thickness obtained by different approaches will not be exactly the same (Israels, Scheutjens et al. 1993).

There is a general lack of understanding of the interactions between the HPGG or borate bound HPGG and solid surfaces in literature. Most of the adsorption tests done at the solid-liquid interface were investigating guar adsorption isotherm on talc or some other minerals. Guar is commonly used in flotation process as flotation depressants and dispersants. There have been some arguments about the driving force of guar adsorption at the solid-liquid interfaces. Jenkins and co-workers found that hydrophobic interactions were dominant in the adsorption process. Hydrogen bonding made only a small contribution to the adsorption, whilst chemical interactions were completely absent (Jenkins and Ralston 1998). Wang and Somasundaran, however, believe that the main driving force for guar adsorption on talc to be hydrogen bonding rather than electrostatic or hydrophobic force. In addition, conformational studies suggest guar adsorb in a very flat conformation on the solid surfaces (Wang and Somasundaran 2007). Laskowski and co-workers suggest that the nature of such interactions between polysaccharide and the mineral surfaces can be categorized as an acid–base interaction, with the polysaccharides behaving as an acid. Mineral surface hydrophobicity was found to have some sort of synergy in the adsorption (Laskowski, Liu et al. 2007).

1.4 Flocculation

The destabilization of colloidal suspensions by salt (i.e. coagulation) or by polymer flocculants (i.e. flocculation) is a phenomenon of industrial importance as well as scientific interest. Colloidal particles suspended in a liquid are subjected to

Brownian motion, fluid flow and external forces. When two colloidal particles experiencing Brownian motion approach each other, they undergo two types of interactions: the particle-particle interactions and hydrodynamic forces mediated by surrounding solvent molecules. These interactions cause the collisions of moving colloidal particles. In a stable colloidal suspension, the electrostatic repulsion between particles prevents aggregation when collision occurs. The aggregation of the suspension is induced by the addition of salt (i.e. coagulation) or polymer flocculant (i.e. flocculation) which will cause the colloidal suspension to become unstable. In general, flocculation, one of the most important methods to separate solids from an aqueous media, is often defined as the gathering together of small masses into larger flocs via polymer.

In terms of the destabilizing mechanism of colloidal system with dissolved polymer, three different regimes are distinguished- bridging flocculation, depletion flocculation (phase separation) and incipient flocculation. Bridging flocculation occurs when the flocculant polymer chain (in a good solvent) has a tendency to be adsorbed onto the surface of colloidal particles. However, the surfaces will be sterically stabilized by the presence of adsorbed polymer layers if the surface is fully covered with adsorbing polymers. Depletion flocculation is observed when the dissolved polymer has non-adsorbing properties. Exclusion of polymers from the space between particles will reduce the osmotic pressure in the space and this reduction cause an attractive force between particles. Incipient flocculation is induced when the medium solvency of the sterically stabilized suspension is reduced greatly to

the condition of poor solvency. This is normally achieved through temperature change or the addition of non solvent medium. The attractive forces observed in the latter two cases are weak and the process can be regarded as reversible. However, as for the process of bridging flocculation, the addition of polymers will push the system far away from equilibrium where dynamic factors are crucial to predict the flocculation performance (Adachi 1995).

The total potential energy of interactions as a function of the distance of separation of two electrostatically stabilized particles is shown in Figure 1-6. As described by the DLVO theory, the total interaction energy is obtained from the combined effect of the Van der Waals attraction and the electrostatic double layer repulsion. This theory assumes that the effect of two forces is additive. And generally one maximum (energy barrier) and one minimum (potential well) can be identified in the total potential energy diagram. If the height of the primary maximum or energy barrier is large enough ($\geq 25kT$), the rate of coagulation of the particles is so slow that the system displays long-term stability. Although it is energetically favorable for particles to come into close contact, a large energy barrier must be overcome first. The depth of the primary minimum or potential well, if sufficiently large, it can give rise to coagulation.

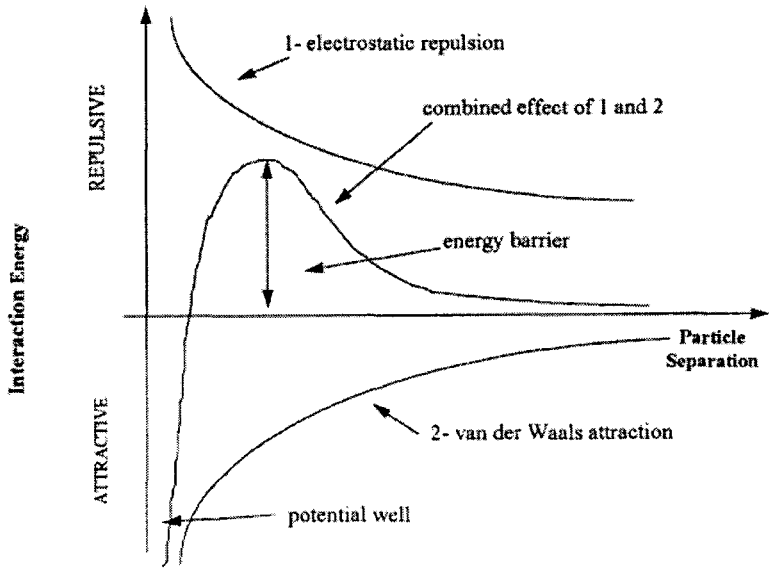

Figure 1-6 Schematic representation of the total potential energy vs distance of separation for a pair of electrostatically stabilized particles(Thomas, Judd et al. 1999).

Flocculation can be induced by eliminating the electrical repulsion (i.e. charge neutralization), adding another force that strongly pulls the particles together, or the addition of a polymer chain that can attach to several particles bridging them together (bridging flocculation). Charge neutralization (Figure 1-7) refers to overcoming electrostatic repulsion between particles and the particles will aggregate due to the attractive Van der Waals forces. As mentioned before, this can be achieved by the addition of an excess of salt that compresses the electrical double layer and lowers the energy barrier to induce collisions. For a charged water soluble polymer, polyelectrolyte, to work as a flocculant in a charge neutralization mechanism, the polymer charge has to be opposite to that of the colloidal particles. The greater the charge density, which is the amount of charged units along the polymer chain, the higher the ability of the polymer to flocculate the particles by neutralizing the charge

on the particle surfaces. At the optimum flocculation conditions the zeta potential of the particles is expected to approach zero, meaning complete neutralization.

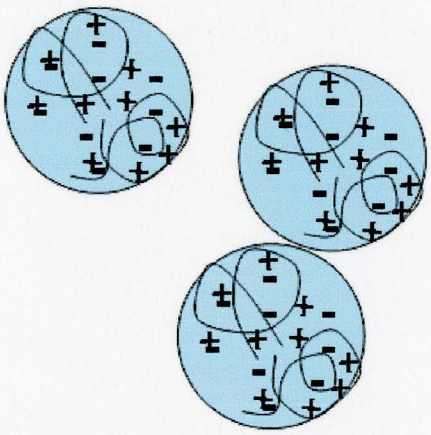

Figure 1-7 Schematic illustration of flocculation by charge neutralization mechanism.

In fact, it is rare to have a polymer system where the flocculation mechanism is solely charge neutralization. A one to one matching of the configuration of the polymer charges to the distribution of charges on the particle surface is physically impossible. This has led to the development of electrostatic patch mechanism (Figure 1-8). Adsorbed polymers will form patches of opposite charges on the particle surface and these domains of different charges will allow for the strong electrostatic attractions between the positively charged areas and negatively charged areas of the particles to form flocs. The electrostatic interactions that hold the particles together can be easily sheared, but they can be easily re-formed as well.

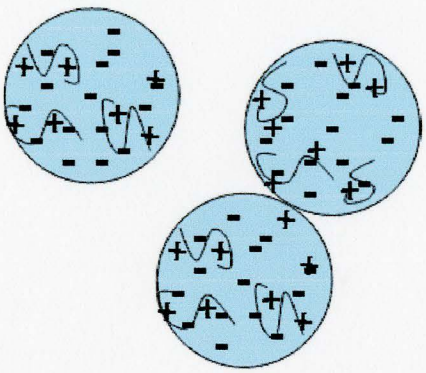

Figure 1-8 Schematic illustration of flocculation by electrostatic patch mechanism.

The configuration of polymer adsorbed onto the particle surface is crucial for electrostatic patch mechanism to work and this is well explained for low to medium molecular weight charged homopolymers. The electrostatic patch mechanism explains systems of highly charged, low molecular weight polymers. For the polymers with high molecular weight, the polymer chain may be too long to assume a flat configuration on the surface and some loops and trains of the adsorbed polymer chain may extend into solution promoting bridging the particles together (Figure 1-9).

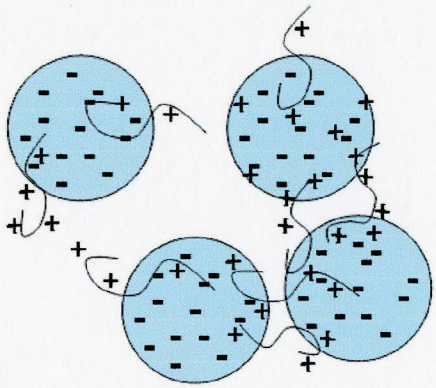

Figure 1-9 Schematic illustration of flocculation by bridging mechanism.

If too much polymer is added to the suspension, the entire particle surfaces will be covered with the polymer and the polymer chains will not be able to find a vacant domain to adsorb onto another particle (Figure 1-10). The particles will now be electrostatically and sterically stabilized (i.e. electrosteric stabilization) by this charged polymer layer and flocculation cannot occur. Therefore there is a range of polymer concentration that effective flocculation performance is obtained in the suspension. According to the concept of "half surface coverage" introduced by La Mer at the first time, optimum flocculation occurs when approximately 50% the surface area is covered by the flocculant (Mer and Healy 1963). And the optimum flocculant dosage will depend on the number of particles in suspension and the surface area of these colloid particles. Unlike the other flocculation mechanisms mentioned previously, the flocs formed by bridging flocculation are large and resistant to shear forces.

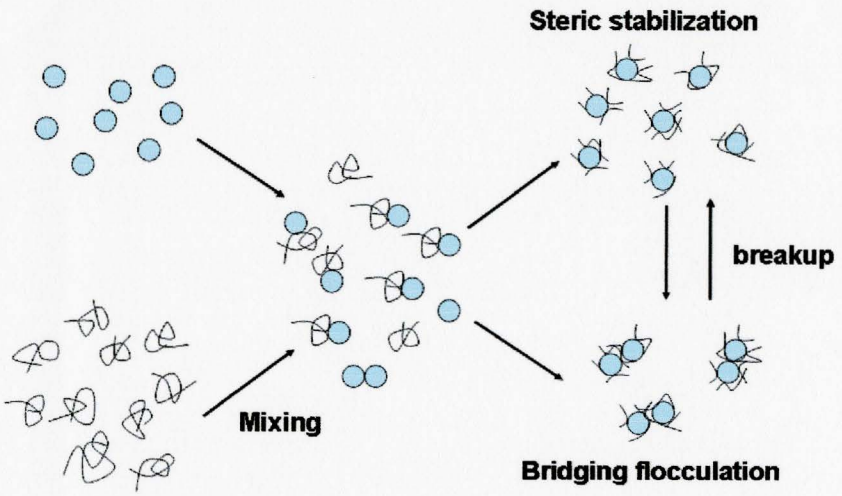

Figure 1-10 Schematic diagram of bridging flocculation with adsorbed polymer.

The flocculation mechanism that explains most experimental data using polymers is bridging flocculation. The molecular weight of most polymeric flocculants is high and thus they are mostly of comparable dimensions to the colloidal particles. A few segments of the polymer chain are attached to the particle surface while the rest of the polymer extends into the bulk solution. The polymer chain is long enough to span over the electric double layer of the particle promoting a point of attachment to another particle. If the same polymer chain becomes attached to more than one particle, these particles are thus bridged together by the polymer. As expected low molecular weight polymers are not effective bridging flocculation agents as the polymers can not reach the distance of several particles. Nonionic polymers such as poly(ethylene oxide) with a high molecular weight are effective flocculants in bridging flocculation.

The bridging flocculation consists of several elementary processes and they can be easily illustrated in Figure 1-10. These are:

(1) Dilution of the flocculant into a solution.

(2) Collision between colloidal particles.

(3) Diffusion of polymer flocculant towards the surface of colloidal particles.

(4) Reconformation of adsorbed polymer on the surface of colloidal particles.

(5) Formation of a "bridge" between colloidal particles.

(6) Rearrangement and breakup of the structure of a floc.

A typical example of the bridging flocculation is shown in Figure 1-11 (Lu and Pelton 2001). Lu et al. used high molecular weight poly(ethylenen oxide) (PEO)

to flocculate polystyrene latex particles.

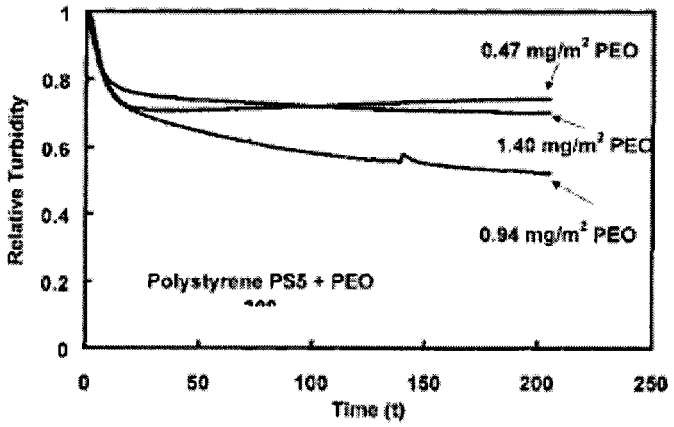

Figure 1-11 Relative turbidity of PS5 polysyrene latex as a function of time (s) from the addition of PEO 309. The labels give the PEO concentration expressed as mass/latex surface area. [PS5] = 0.2 g/L, and [NaCl] = 0.001 mol/L (Lu and Pelton 2001).

It is demonstrated in Figure 1-11 that the flocculation extent of PS5 as a function of time for three different PEO concentrations. The reduction of relative turbidity the suspensions in all cases proved the presence of flocculation. Relative turbidity is a measure of the concentration of unflocculated latex; lower relative turbidity means better flocculation. As shown in Figure 1-11, the minimum relative turbidity, which is a measure of the extent of flocculation, was greater than 0.5 indicating poor flocculation.

Figure 1-12 shows the relative turbidity of the latex as a function of the flocculant polymer concentration. The polymer concentrations over certain range yield the minimum relative turbidity values. Higher polymer concentrations caused flocculation to deteriorate and latex particles to be sterically stabilized again (Xiao, Pelton et al. 1995).

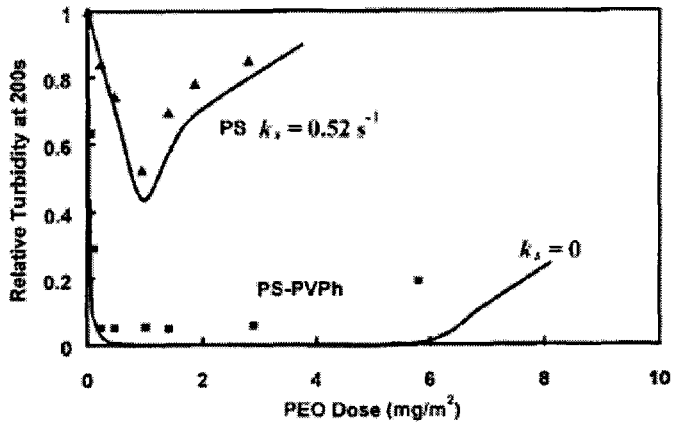

Figure 1-12 Influence of PEO 309 dose on latex flocculation. The solid lines denote model results. [PS5] and [CPS5] = 0.2 g/L, and [NaCl] = 0,001 mol/L (Xiao, Pelton et al. 1995).

A couple of papers introduced the application of chemically modified guar as flocculant. Singh et al. synthesized guar gum grafted polyacrylamide (GG-*g*-PAM) and hydroxypropyl guar gum grafted polyacrylamide (HPGG-*g*-PAM) and studied the flocculation characteristics of the graft copolymers in kaolin, iron ore, and silica suspensions. It is observed that guar gum exhibits better performance than hydroxypropyl guar gum in all three suspensions. For the graft copolymers, HPGG-*g*-PAM shows superior performance to GG-*g*-PAM and even various commercially available flocculants in those three suspensions (Nayak and Singh 2001). They reported that the copolymer HPGG-*g*-PAM had superior flocculation efficiency to unmodified HPGG as well as polyacrylamide homopolymer. In Figure 1-13 the flocculation properties of cationic guar in silica suspension were compared with some of the commercially available flocculants. The results show that compared to the other commercial flocculants a better flocculation performance for cationic guar

is observed (Singh, Pal et al. 2006).

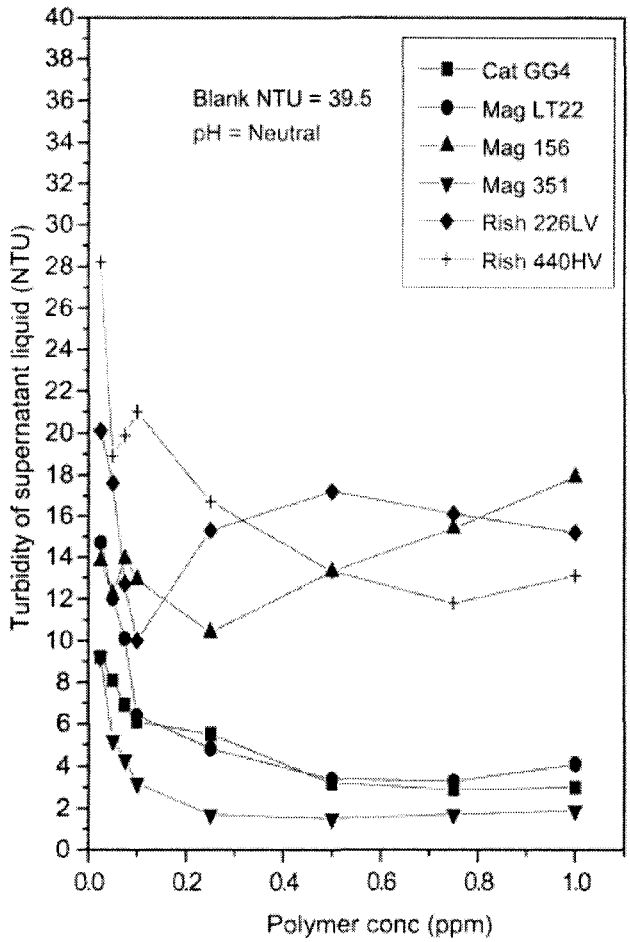

Figure 1-13 Jar test result in silica suspension using Cat GG4 and commercial flocculants (Singh, Pal et al. 2006).

1.5 The Tear Film

The exposed part of the ocular globe is covered by a thin fluid film, the preocular tear film. The presence of a continuous and stable tear film over the ocular surface is crucial for the well-being of the cornea epithelium and thus good vision. In addition to protecting the delicate ocular surface, the tear film also contains substances with antibacterial properties, providing defense against bacterial invasion

(Holly 1993).

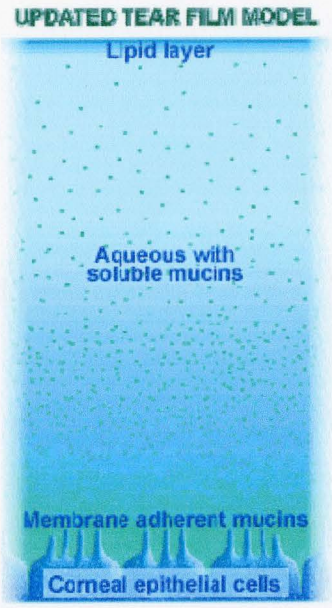

Figure 1-14 Schematic representation of tear film structure.

Holly et al. described the eye tear film, the thickness of which is typically 4 to 10 μm, as a three-layered structure- the outmost lipid (oily) layer at the tear/air interface, the aqueous layer that makes up 90% of the tear film volume; and the deep mucin layer that coats the corneal surface. The author also proposed a model of the tear film as a coacervate, in which goblet cell mucin was present as a gel in the deepest layer that was fixed to the cornea while soluble mucin was present in the overlying aqueous layer (Holly 1987). Schematic representation of tear film structure is shown in Figure 1-14. Studies by Holly suggested that the native corneal epithelium was hydrophobic, and hence water repellent, but was rendered hydrophilic by the application of goblet cell mucin to its surface during blinking. It was obtained that the mucin not only works as a barrier to bacterial pathogens but also makes ocular surface

hydrophilic.

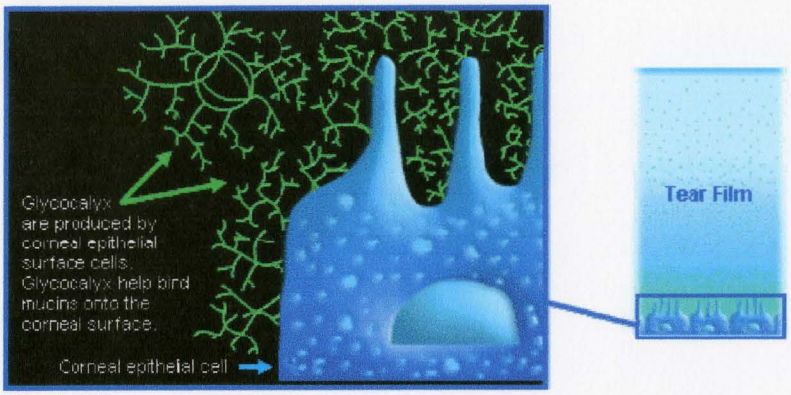

Figure 1-15 Schematic representation of glycocalyx that are formed by corneal epithelial surface cells (http://www.systane.com/eyecare-professional/Tear-Film.asp).

It is believed that glycocalyx, which are long chain molecules produced by corneal epithelial surface cells, help anchor mucins onto the corneal surface (Figure 1-15). Any damages to the glycocalyx and corneal surface cells may cause the loss the mucins that are bound onto the eye's surface, which in turn makes surface hydrophobic and repel water. As shown in Figure 1-16, this can result in the tear film destabilization and break-up, exposing the injured cornea to the air and bacterial pathogens (Paulsen and Berry 2006). Ultimately, the patient is diagnosed of having dry eyes.

A number of approaches exist for treating dry eyes. One common approach has been to supplement the tear film with artificial tear solutions on a regular basis. The current commercially-available products for treatment of dry eyes mostly contain water-soluble polysaccharides, such as carboxymethyl cellulose, sodium hyaluronate

and hydroxypropyl guar (Ubels, Clousing et al. 2004; Johnson, Murphy et al. 2006). These polymers render the solutions more viscous and thus less easily shed due to the motion of eyelid.

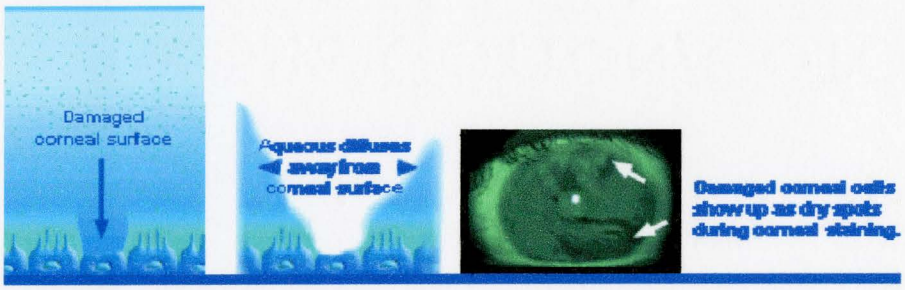

Figure 1-16 Schematic representation of damaged corneal surface causing tear film instability (http://www.systane.com/eyecare-professional/Tear-Film.asp).

Although these products have met with some success in some cases, problems in the treatment of dry eye remain. The major challenge is how to extend the products' duration in the eye since they are only temporarily effective and repeated application of the products is required. Studies of solution properties of the polymers used in these artificial tear products show that with increasing viscosity the products are able to extend the products' duration in the eye (Lu, Kostanski et al. 2005). However, properties of the polymers at the solution-solid interfaces haven't been extensively studied and their effects on those products' performance in treating dry eye are poorly understood. The purpose of this work is to investigate HPGG's role in treating dry eye from a perspective of solution-solid interfaces.

Chapter 2 Experimental Methods

This chapter describes the approaches used for the study of adsorption and flocculation properties of HPGG and HPGG/Borate, including electrophoresis, dynamic light scattering, and Ultraviolet-visible Spectroscopy.

2.1 Transmission electron microscopy (TEM)

What people can see with a light microscope is limited by the wavelength of light. TEMs use electrons as "light source" and thus those much lower wavelength makes it possible to get a resolution a thousand times better than with a light microscope. How A TEM works can be explained by comparing it to a slide projector. A projector shines a beam of light through the slide and it is affected by the structures and objects on the slide as the light passes through. These effects cause only certain parts of the light beam being transmitted through certain parts of the slide. This transmitted beam is then projected onto the viewing screen and an enlarged image of the slide is formed. TEM works in the same way except that they shine a beam of electrons (instead of the light) through the specimen (instead of the slide). Whatever part is transmitted is projected onto an imaging screen, a fluorescent screen in most TEMs, for the user to see. A more technical explanation of a typical TEMs workings is as follows (refer to the diagram below):

1. The electron gun at the top produces a stream of monochromatic electrons.

2. This stream is focused to a small, thin, coherent beam by the use of condenser lenses, normally two lenses. The first one, which is usually controlled by the "spot

size knob", determines the spot size and the general size range of the final spot that strikes the sample. The second one, which is usually adjusted by the "intensity or brightness knob", actually changes the size of the spot on the sample from a wide dispersed spot to a pinpoint beam.

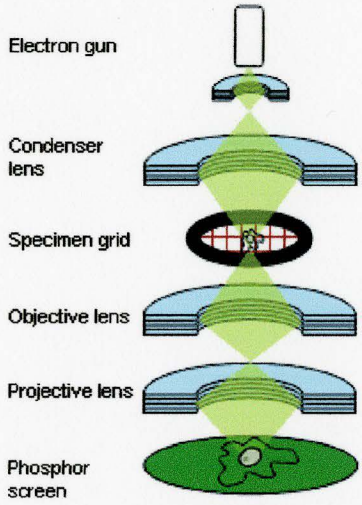

Figure 2-1 Schematic representation of a typical Transmission Eelectron Microscopy (www.steve.gb.com/science/electron_microscopy.html).

3. The beam strikes the specimen and parts of it are transmitted through the specimen.

4. This transmitted beam is focused by the objective lens into an image

5. The image is passed down the column and enlarged through the projective lenses.

6. The image strikes the phosphor image screen or a layer of photographic film, or to be detected by a sensor such as a CCD camera so the user can see the image. The darker areas of the image represent those areas of the sample that are thicker or denser so fewer electrons were transmitted through. The lighter areas of the image represent those areas of the sample that are thinner or less dense so more electrons were

transmitted through.

The TEM is used largely in both material science and the biological sciences. For biological specimens, the maximum specimen thickness is about 1 micrometer. To withstand the instrument vacuum, biological specimens are usually held at liquid nitrogen or fixed by a negative staining material like uranyl acetate. The specimens in material science tend to be naturally resistant to vacuum, but they must be prepared as a thin foil so thin enough for the electron beam to penetrate. On the other hand, for materials that have dimensions small enough to be electron transparent, such as nanoparticles or nanotubes, specimens can be quickly prepared by the deposition of a dilute sample containing the studied materials onto support cooper grids. Normally, the specimen is dispersed in a volatile solvent, such as ethanol or water, ensuring that the solvent evaporates rapidly before a sample can be analyzed quickly.

The TEM specimen preparation in this work consists in transferring a suspension of the particles in deionized water to a carbon coated grid and letting the water evaporate. The suspension is diluted from latex produced in our lab as described later in materials section and ultrasonicated before transferring to the grid.

2.2 Dynamic Light Scattering

Dynamic light scattering (DLS), also known as Photon Correlation Spectroscopy (PCS), is a well established technique for measuring particle size over the size range from a few nanometers to a few microns. The concept is based on the idea that small particles in a suspension move in a random pattern, termed "Brownian

Motion". The larger particles move more slowly than the smaller ones if the temperature is the same. When a coherent source of light with a known frequency, like a laser, is directed at the moving particles, the light is scattered, but at a different frequency. This change of frequency is quite similar to the change in frequency or pitch one hears when a train approaches and finally passes. The concept is basically the same for light when it interacts with small moving particles. For the purpose of measuring particle, the shift of light frequency is related to the size of the particles causing the shift. Because of their higher average velocity, smaller particles result in a greater light frequency shift than larger particles. The difference in the frequency of the scattered light among particles of different sizes is used to determine the sizes of the particles present.

As expressed in the intensity correlation function C, the motion of the particles in the solution changes the coherence of the scattered light. A digital correlator is used to compute the autocorrelation function. By examining their autocorrelation the time variation of the scattered intensity is analyzed. A diffusion coefficient is thus derived and particle size can be calculated from the measured diffusion coefficient (Brookhaven Manual).

$$C(\tau) = Ae^{-2\Gamma\tau} + B \qquad (2\text{-}1)$$

Equation 2-1 gives $C(\tau)$, the autocorrelation function. A and B are instrument specific constants and Γ, the decay rate is given by the following equation.

$$\Gamma = q^2 D \qquad (2\text{-}2)$$

Where q is the scattering vector and D is the diffusion coefficient.

$$Q=4\pi n\sin(\theta/2)/\lambda \quad (2\text{-}3)$$

and

$$D=k_B T/3\eta d \quad (2\text{-}4)$$

where n is the refractive index,

θ is the scattering angle,

λ is the laser wavelength,

k_B is the Boltzmann's constant,

T is the temperature in Kelvin,

η is the liquid viscosity,

d is the particle diameter.

Generally speaking, dynamic light scattering yields either an average diffusion coefficient or a distribution function of diffusion coefficients for polydisperse samples. By assuming Stokes law (equation2-4), which is applicable for dilute suspensions of spheres, the corresponding hydrodynamic diameters are obtained. The diameter that is measured in Dynamic Light Scattering is called the hydrodynamic diameter and refers to how a particle diffuses within a fluid. The diameter obtained by this technique is that of a sphere that has the same translational diffusion coefficient as the particle being measured, which may not be perfectly sphere. The translational diffusion coefficient depends not only on the "core" size of the particle, but also on any surface structure, as well as the concentration and type of ions in the solution. This means that the size can be more or less larger than that measured by electron microscopy, for example, where the particle is analyzed in a vacuum environment that is from its native environment.

2.3 Ultraviolet-visible Spectroscopy

Ultraviolet-visible spectroscopy or ultraviolet-visible spectrophotometry (UV-Vis) involves the spectroscopy of photons in the UV-visible region. It uses light in the visible and adjacent near ultraviolet (UV) and near infrared (NIR) ranges. In this region of the electromagnetic spectrum, molecules undergo electronic transitions. UV-Vis spectroscopy is widely used as an analytical technique for two reasons. First it can be used to identify some functional groups in molecules and secondly, it can be used for assaying, such as the determination of the trace metal content in alloys or the small amount of a certain drug reaching various parts of the body.

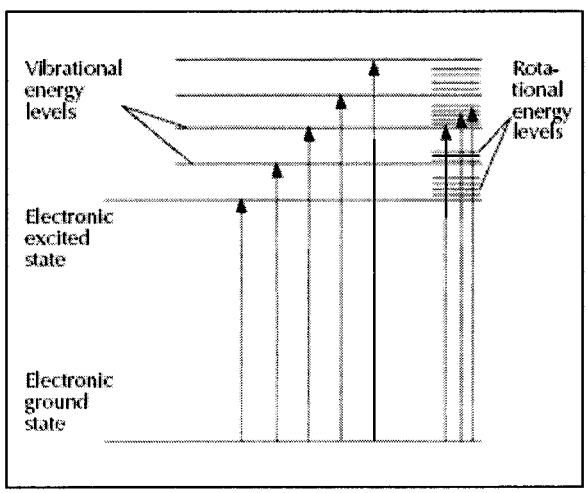

Figure 2-2 Diagram of electronic transitions.

The adsorption of electromagnetic radiation by a molecule leads to the excitation of electrons from their normal (ground) states to a higher energy (excited) states. The energies of the orbitals involved in electronic transitions have fixed values.

When sample molecules are exposed to light with an energy that matches a possible electronic transition within the molecule, some of the light energy will then be adsorbed so the electron is excited to a higher energy orbital. The resulting spectrum is often presented as a graph of absorbance versus wavelength. Though the energy is quantized, absorption peaks in a UV-Vis spectrum are rarely sharp peaks. Instead the spectrum has broad peaks and this is due to vibrational and rotational energy levels available to absorbing materials.

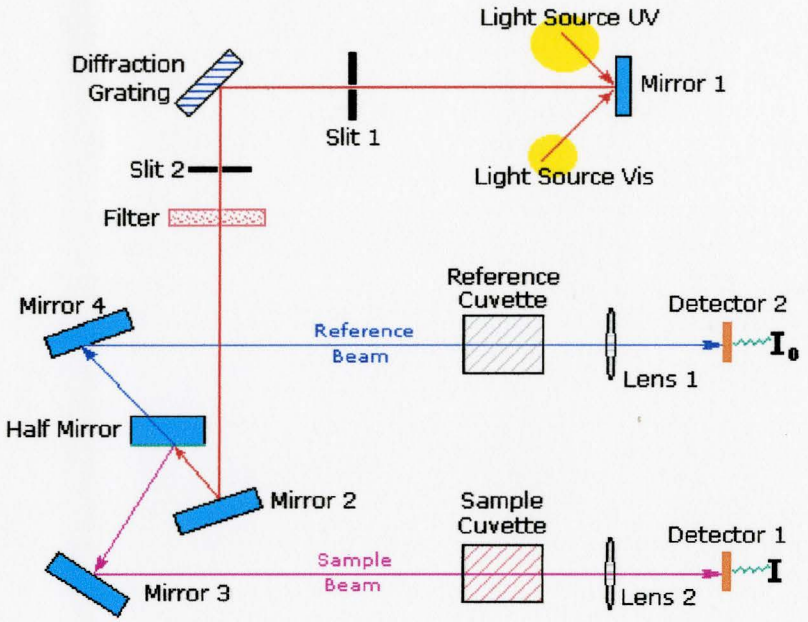

Figure 2-3 Schematic illustration of components of a typical spectrometer.

Above is a diagram showing the components of a typical spectrometer and the functioning of this instrument. A beam of light a visible or UV light source is separated into its component wavelengths by diffraction grating. Each monochromatic beam is then split into two equal intensity beams by a half-mirrored device. The

sample beam passes through a small transparent cuvette containing a solution of the sample in a transparent solvent. The reference beam, on the other hand, passes through an identical cuvette containing only the solvent. The intensities of both sample and reference light beams are then measured by electronic detectors. The intensity of the reference beam, which is defined as I_0, should have little or no light absorption. The intensity of the sample beam, however, is defined as I. The difference between I_0 and I may be plotted on a graph versus wavelength. Transmittance ($T=I/I_0$) or absorbance ($A=\log_{10} I_0/I$) is used to study absorption. The commonly observed range for absorbance is from 0 (100% transmittance) to 2 (1% transmittance). The wavelength of maximum absorbance, λ_{max}, is a distinct value. Different samples may have very different absorption maxima and absorbances.

According to the Beer-Lambert law, the absorbance of a solution is directly proportional to the sample concentration in the solution. Therefore UV-Vis spectroscopy is usually used in a quantitative way to determine concentrations of an absorbing species in solution.

$$A = -log_{10}(I/I_0) = \varepsilon C L$$

Where A is the measured absorbance, I_0 is the intensity of reference beam or incident light in some cases at a given wavelength, I is the intensity of sample light beam, L the pathlength through the sample, and C the concentration of the absorbing species. For each species and wavelength, ε is a constant known as extinction coefficient and it is a fundamental molecular property in a given solvent at a particular temperature and pressure.

2.4 Electrophoresis

Generally, electrophoresis refers to the motion of dispersed particles relative to a fluid under the influence of an electric field that is space uniform. We all know that the viscous fluid adjacent to the particles surface assumes the same velocity as the surface, yet it is not the case for the fluid at a distance from the surface. Thus, it is expected that relative motion between the particles and the counterions occurs if we induce motion of the particles in an electrical field. The point in the electrical double layer δ where the surrounded medium begins to flow is defined as the location of the zeta potential.

Particles dispersed in fluid almost always carry an electric surface charge to stay stable. An electric field exerts electrostatic force on the particles through these charges so they migrate and thus electrophoresis occurs. The electric force is balanced with hydrodynamic friction, which affects all moving bodies in viscous fluids. The particle will then reach a steady state velocity in which electrical force and viscous force are equal. We can thus estimate the velocity using Stoke's law:

$V = F / 6\pi\eta R$

in which F is the external force induced by the electrical field. The speed of the moving bodies V is proportional to the electric field strength E . Electrophoretic mobility μ_e is thus introduced as coefficient of proportionality between particle speed and electric field strength:

$\mu_e = v / E$

This quantity is the primary value determined in an electrophoresis experiment.

2.5 Colorimetric Assay

The anthrone method is an example of a colorimetric method of measuring the concentration of the total sugars in a sample. Sugars react with the anthrone reagent under acidic conditions, yielding a greenish blue color. Mixed with sulfuric acid and the anthrone reagent first, the sample is then boiled until the reaction is completed. The mixture is then allowed to cool down and its absorbance at 620 nm is measured. The relationship between the absorbance and the amount of sugar present in the sample is found to be linear. The Phenol-Sulfuric Acid method is another widely used colorimetric method for determining the total concentration of carbohydrates present in samples. The clear solutions of the carbohydrates turn a yellow-orange color as a result of the interaction between the carbohydrates and the phenol after mixing them. The absorbance at 420 nm is proportional to the carbohydrate concentration in the sample. For both of them, it is necessary to prepare a calibration curve using a series of standards of known carbohydrate concentration.

Not only monosaccharides, but also oligosaccharides and polysaccharides concentrations in the samples have been successfully determined by anthrone method, with slight modification in some cases (Viles and Silverman 1949; Blakeney and Mutton 1980).

2.6 Materials

Guar and Hydroxypropyl guar gum (HPGG) with a degree of substitution of 0.36 and a molecular weight of 1.2-1.5 $\times 10^6$ Da was obtained from Alcon laboratories.

Styrene, 2,2'-azobis(2-diisobutyramidine) dihydrochloride (AIBA) and potassium persulfate (PP) were purchased from Sigma-Aldrich. Anionic and cationic polystyrene (PS) latexes were prepared by emulsifier-free emulsion polymerization of styrene using either an anionic PP or a cationic AIBA radical initiator (Goodwin, Ottewill et al. 1979). The polymerization reactions were all carried out in a 250 ml round-bottomed, three-necked flask. Normally, a total reaction volume of 120 ml of liquids was used. A typical preparation of polystyrene latex particles with potassium persulfate as the initiator (PSL-A) was carried out in the following manner. A glass stirrer fitted into a PTFE guide was inserted into the middle outlet and then attached to a tachometer. One of the side outlets of the flask was equipped with a water-cooled reflux condenser. The flask was immersed up to the neck in a thermostat oil bath with a controlled temperature of 70±1℃ during the polymerization reaction. Nitrogen was bubbled through the water in the flask to remove oxygen from the system using the other side outlet of the flask. The stirrer was adjusted to 350 revolutions per minute. After stirring for half an hour with nitrogen passing through the flask, 8 g styrene was added and then left for 10 minutes to achieve temperature equilibrium and effective mixing. 80 mg of the initiator, dissolved in 20 ml of water, was then added to the flask. After 12 hours the flask was removed from the oil bath and allowed to cool for a few minutes. The cationic polystyrene latex with AIBA as the initiator (PSL-C) was produced in a similar manner. Table 2-1 gives the detailed recipes used in this work.

The charged polystyrene latex particles (PSL-A, PSL-C) were centrifuged and redispersed in Millipore-water three times before use. Hydrodynamic average particle

sizes of the particles were determined to be 302.4 nm with a polydispersity of 0.096 (PSL-C) and 840.8 nm with a polydispersity of 0.067 (PSL-A) by DLS.

Table 2-1 Polymerization reaction recipe and properties of formed colloidal particles (EM: Electrophoretic mobility).

Latex	Styrene / g	Initiator / mg	Water / ml	Diameter / nm	EM / $10^{-8}m^2/Vs$
PSL-A	8.0	80.0	120	840.8±23	-2.10
PSL-C	8.0	80.0	120	302.4±16	+2.30

Borax ($Na_2B_4O_7 \cdot 10H_2O$), phenylboronic acid (PBA), methylboronic acid (MBA), D-Fructose, anthrone and concentrated sulfuric acid were purchased from Sigma- Aldrich and generally used as received.

2.7 Adsorption

Solutions of HPGG samples with different concentrations were prepared by dissolving polysaccharide in Milli-Q water then, after stirring, ionic strength was adjusted as needed. In a typical adsorption experiment in the presence of borax, 50 ml HPGG solution with boron concentration of 0.03M was stirred in a 250 ml beaker for 24h before use. The pH values of the solutions were adjusted by 0.1M NaOH and 0.1M HCl solutions to 7.4. The ionic strength was adjusted by adding 0.1M sodium chloride in all adsorption experiments except mentioned especially in some cases. Under continuous stirring, 0.2 ml anionic polystyrene latexes (solid concentration 50

g/L) were then introduced to the mixture. Preliminary kinetic experiments indicated that within two hours adsorption equilibrium was attained. Hence in all adsorption tests, the time of equilibration was fixed at 6h. After 6h stirring at controlled temperature, the samples were centrifuged using a Beckman Allegra™ 25R Bench Centrifuge at 6,000rpm for 30min and a part of supernatant, containing non-adsorbed HPGG, was taken. HPGG concentration in the supernatant was determined by anthrone method using DU® 800 UV/Visible Spectrophotometer at a wavelength of 625 nm. The supernatant to be tested (1.0ml) was first measured into a clean, dry 15×125 mm. Pyrex test tube and 4.0 ml of 0.2% (g/ml) anthrone dissolved in concentrated sulfuric acid were added afterwards. The tube was then shaken to achieve complete mixing. The heat produced by mixing acid and water appeared to be a necessary part of the reaction and it turned out to be enough for the reaction to take place completely. After approximately 10 to 15 minutes, the tube was air-cooled completely. Under controlled conditions the amount of green color produced is proportional to the polymer content in the supernatant. The absorption of this newly formed green solution was measured at 625 nm. A calibration curve using a series of standards of known HPGG concentration was prepared to relate light absorption to polymer concentration. A linear calibration curve relating the absorbance of supernatant added with anthrone as a function of the HPGG concentration was obtained with UV/Visible Spectrophotometer (Figure 2-4).

The adsorbed amount (Γ) was calculated from the difference between the initial polymer concentration and the concentration in the supernatant by anthrone

method. The absorbance reading at 625 nm obtained from UV/Visible Spectrophotometer were converted to concentration from calibration curve and the amount of HPGG adsorbed per unit surface area of anionic polystyrene latex particle surface was calculated assuming that the particles are perfectly uniform and all the surface areas are available for adsorption.

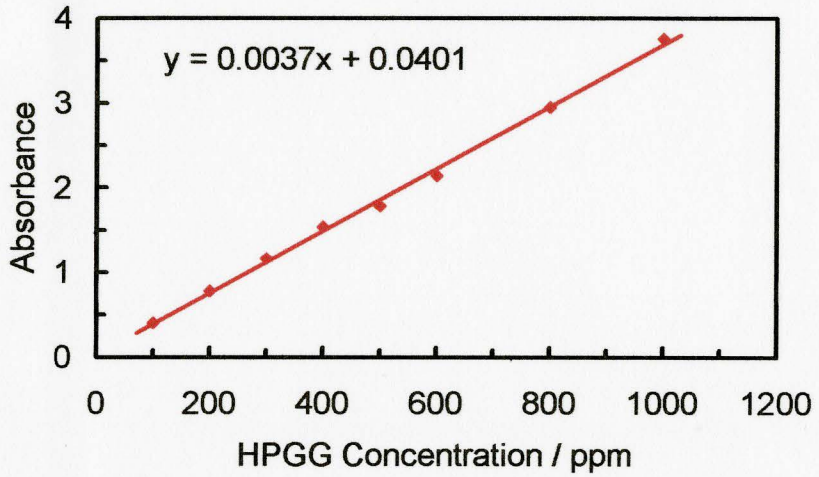

Figure 2-4 Calibration curve for absorbance at 625 nm vs. HPGG concentration.

The electrophoretic mobility of the mixture was measured using a Brookhaven ZetaPALS (USA) instrument at 25°C in PALS (phase analysis light scattering) mode (PALS software version 2.5). The reported mobility was the average of 10 cycles with each consisting of 20 scans. Measurements were made on the anionic latex particles alone and in the presence of HPGG or HPGG-borate at equilibrium concentrations. In another set of experiments, adsorption experiments were done in the absence of borate.

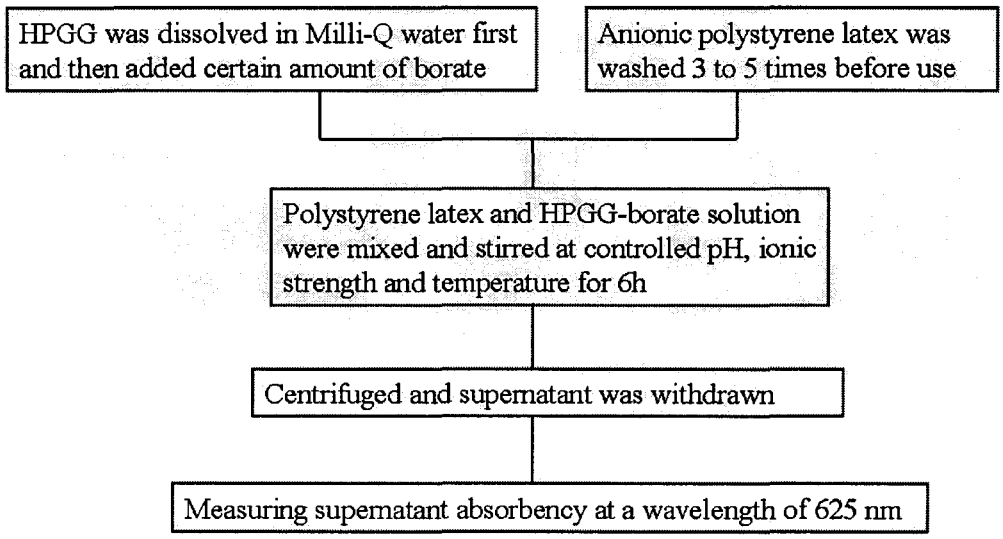

Figure 2-5 Adsorption process employed in this study.

2.8 Flocculation

Solutions of HPGG samples with different concentrations were prepared by dissolving polysaccharide in Milli-Q water then, after stirring, ionic strength was adjusted as needed. In a typical flocculation experiment in the presence of borate, HPGG solution added with 0.03M borax buffer was stirred for 24h before use. The pH values of the solutions were adjusted by 0.1M NaOH and 0.1M HCl solutions. Under continuous stirring, 0.2 ml cationic polystyrene latexes (solid concentration 50 g/L) were then introduced to the mixture. Preliminary kinetic experiments indicated that within an hour flocculation equilibrium was attained. Hence in all flocculation tests, the time of equilibration was fixed at 2h. After 2h stirring at controlled temperature, the suspension was let stand for 12h to settle down the floccs. The degree to which suspensions of cationic polystyrene latex particles were flocculated

was analyzed using DU® 800 UV/Visible Spectrophotometer at a wave length of 500 nm. The turbidity of a colloidal dispersion at a given wavelength, λ, depends on the particle number concentration, the particle radius, its refractive index, and the refractive index of the medium. When others remain constant, the turbidity appears to be a function of particle number concentration (Jeffrey and Ottewill 1988). Therefore, turbidity is mostly employed for the determination of flocculation extent. In this study absorbance of supernatant were measured at 500 nm using UV/Visible Spectrophotometer. The absorbance of untreated colloidal suspension exposed to the same stirring conditions but without HPGG addition was measured simultaneously to take into consideration turbidity decrease due to flocculation. Residual turbidity in this work was calculated as the ratio of light absorbance in the presence of HPGG over that in the absence of HPGG (Bratskaya, Avramenko et al. 2006).

The electrophoretic mobility of the mixture was measured using a Brookhaven ZetaPALS (USA) instrument at 25°C in PALS (phase analysis light scattering) mode (PALS software version 2.5). The reported mobility was the average of 10 cycles with each consisting of 20 scans. Measurements were made on the cationic latex particles alone and in the presence of HPGG or HPGG-borate at equilibrium concentrations. In other sets of experiments, flocculation experiments were done in the presence of phenylboronic. For suspensions with optimum flocculation induced by borax, the pH values were adjusted by NaOH and HCl to study its effect on residual turbidity and electrophoretic mobility. In addition, various amount of D-Fructose was added to the suspension with optimum flocculation and its

influence on HPGG-borate polyelectrolyte chain charge density was calculated (refer to for details). The relationship between polymer chain charge density and flocculation efficiency was studied as well.

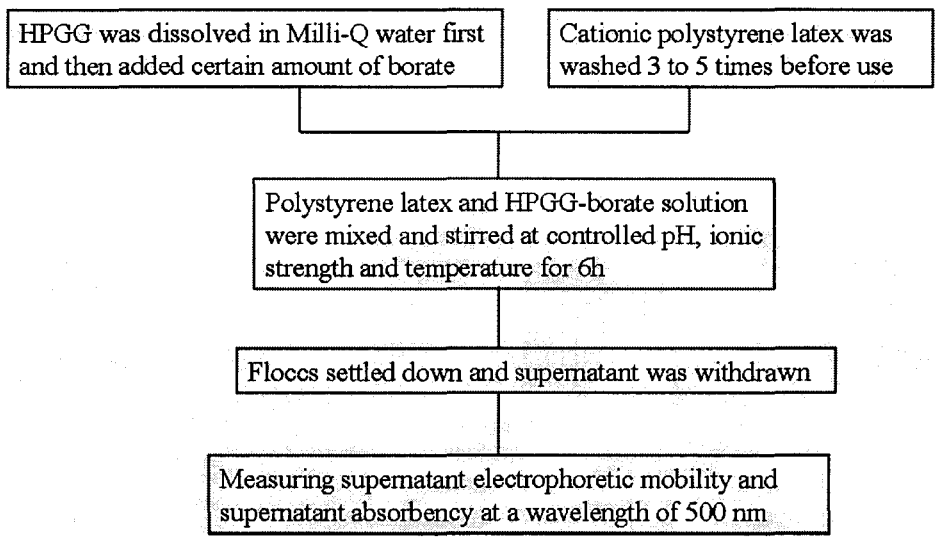

Figure 2-6 Flocculation process employed in this study.

Chapter 3 Adsorption

In this chapter, the adsorption behavior of HPGG alone and in the presence of borate is presented and the adsorption mechanism is discussed. In addition, the electrophoresis results of the bare hard particles and soft particles that were covered with HPGG or HPGG/Borate are described and compared.

3.1 Results

3.1.1 Adsorption isotherm

HPGG adsorption density on anionic polystyrene latex particles (Figure 3-1) surfaces were determined by the anthrone method. Figure 3-2 shows that HPGG adsorption on anionic polystyrene latex (PSL-A) does not quickly reach a single plateau in the adsorbed density with increasing polymer solution concentration, which means it is not a high affinity adsorption. In addition, the data in Figure 3-2 show that there is not much difference in the adsorption density for experiments done at 25℃ and 35℃, which indicates that HPGG adsorption on PSL-A is temperature insensitive over the range under study in this work. The maximum HPGG adsorption density on PSL-A was shown be around 0.10 mg/m^2 and 0.13 mg/m^2 at 25℃ and 35℃, respectively.

HPGG bound with either borate or methylboronic acid adsorption isotherm on PSL-A was determined through the similar procedures. It should be noted that the total boron concentrations in borax and methylboronic acid in this study is equivalent.

It is shown in Figure 3-3 that HPGG/borate adsorption on negatively charged particles is not a high affinity adsorption either, adsorption density increasing slowly along with residual concentration of HPGG before leveling off. The average maximum adsorption density values for experiments done with added sodium chloride concentrations of 0.10M and 0M are 0.07mg/m^2 and 0.05mg/m^2, respectively. The data shown in Figure 3-3 demonstrate that maximum adsorption density is increased when adsorption experiments were done with a higher ionic strength. In addition, borax was replaced by methylboronic acid (MBA) to study HPGG/MBA adsorption on PSL-A. HPGG/MBA adsorption isotherms (Figure 3-4) display the similar figure to that of HPGG/borate adsorption. As shown in Figure 3-4, the average maximum adsorption density values for experiments done with added sodium chloride concentrations of 0.10M and 0M are 0.06mg/m^2 and 0.05mg/m^2, respectively. Adsorption of guar on PSL-A in the same conditions as HPGG was studied as well and the results are shown in Figure 3-5. It is found that there is no distinct difference between HPGG and guar adsorption over the concentration range measured.

3.1.2 Electrophoretic mobility

Figure 3-6 shows the electrophoretic mobility of anionic polystyrene latex alone and in the presence of HPGG or HPGG/borate as a function of pH. The electrophoretic mobility of anionic polystyrene latex with residual persulfate groups on the surfaces does not demonstrate any dependence on pH and the values are around -2.0×10^{-8} m^2/Vs from pH 2.5 to pH 12.0. The mobility values of PSL-A added with

HPGG, on the other hand, are less negative and they are all around -0.2×10^{-8} m^2/Vs over the pH range measured in this study. As shown in Figure 3-6, electrophoretic mobility of PSL-A covered with HPGG/borate or HPGG/MBA are both pH-dependent. The mobility values of these two mixtures are around -0.2×10^{-8} m^2/Vs and stable in acidic and neutral conditions. As pH values are increased from pH 7 to pH 10, the electrophoretic mobility values are reduced and appear more negative quickly. When pH values are increased further from pH 10 to pH 12, the mobility values all level off in both cases, which are around -1.1×10^{-8} m^2/Vs and -1.5×10^{-8} m^2/Vs for HPGG/borate and HPGG/MBA, respectively.

3.1.3 Dynamic Light Scattering

The hydrodynamic sizes of polystyrene latex particles alone and in the presence of HPGG and HPGG/borate were investigated using dynamic light scattering. The measurements were done with the suspensions that showed maximum HPGG adsorption on particle surfaces. Total boron molecular concentrations in suspensions with borax and MBA (pKa= 10.7) were 0.03M and pH values were not adjusted. As shown in Table 3-1, the hydrodynamic diameters of bare particles were around 840 nm and after the addition of HPGG that increased to around 1240 nm. For comparison, borax and methylboronic acid (MBA) were also introduced to the mixed suspension of polystyrene particles and HPGG. It was found that the hydrodynamic diameters for the suspensions with borax were reduced by around 100 nm and the diameter values for suspensions with methylboronic acid were around 1200 nm.

Table 3-1 Hydrodynamic diameter size of the bare particles and the ones covered with polymers measured by dynamic light scattering.

Suspension	PSL-A (pH:7.4)	PSL-A & HPGG (pH:7.4)	PSL-A & HPGG/Borax (pH:9.0)	PSL-A & HPGG/MBA (pH:10.5)
Diameter Size /nm	840±23	1240±24	1140±21	1200±26

3.2 Discussion

3.2.1 Adsorption isotherms

The adsorption isotherms of HPGG on anionic polystyrene latex particles surfaces at a pH value of 7.4 and added sodium chloride concentrations of 0.10M at 25 ℃ and 35 ℃ are shown in Figure 3-2. It was found that adsorption density of HPGG at both temperatures increased with increasing polymer concentration in the solution. The isotherms follow Langmuirian behavior and exhibit a gentle rise in the adsorption density at low concentrations and then reach the equilibrium density at HPGG concentration of about 400 ppm.

Electrophoresis results illustrated in Figure 3-5 demonstrate that with the addition of HPGG to polystyrene suspensions the electrophoretic mobility increased from -2.0×10^{-8} m^2/Vs for bare particles to -0.2×10^{-8} m^2/Vs, which is believed to be due to the adsorption of HPGG onto the particle surfaces. The HPGG concentration was such that the adsorption density of the polysaccharide was at its plateau so the

surfaces of the particles were saturated with the polysaccharide. The adsorbed HPGG simply moves the shear plane farther away from the particle surface thus decreasing the magnitude of the zeta potential (Ma and Pawlik 2005; Liu, Feng et al. 2006).

As reported in many studies, guar and its derivatives exhibit high affinity type of adsorption on various mineral surfaces. Liu and Laskowski emphasized the importance of metal impurities on mineral surfaces that can serve as active sites for polysaccharide adsorption (Laskowski, Liu et al. 2007). In this case the adsorption was viewed as metal-polysaccharide complexation facilitated by the *cis*-configuration of the hydroxyl groups of the mannose monomers. And the adsorption, with an adsorption density around 1.0 mg/m^2, can be categorized as a strong acid-base interactions between metal hydroxylated species and polysacchardies, which they claimed to predominantly take place on the hydrophobic faces. The adsorption density on quartz particles rendered hydrophobic via methylation, on the other hand, was found to be around 0.10 mg/m^2. Hydrophobic interactions between the polymer and basal cleavage planes were found to dominate adsorption process on talc, leading to adsorption of the guar onto hydrophobic sites with maximum adsorption densites around 1.0 mg/m^2 (Jenkins and Ralston 1998). Based on the study of the influence of temperature on adsorption, they concluded that dehydration of both the hydrocarbon portions of the guar polymeric chain and the hydrophobic talc surface are the driving forces which control transport, and subsequent adsorption, of the guar from the bulk solution to the hydrophobic surface. In addition, Muller et al. studied adsorption properties of hydrophobically modified carboxymethylpullulans onto polystyrene

latex particles (Simon, Picton et al. 2005). They concluded that hydrophobic interactions between the grafted alky chains and the surface are responsible for the adsorption of the polysaccharides.

In conditions that adsorption tests were done in our work, polystyrene particles were hydrophobic and negatively charged due to sulfate groups on the surfaces. Our adsorption isotherms show that HPGG adsorption onto negatively charged hydrophobic particles is not high affinity type of adsorption. And this adsorption could be explained as the minimization of unfavorable hydrocarbon polymer segments-water and hydrophobic surfaces-water contacts in our work. Not only the adsorption mechanism but also the adsorption densities of our results agree well with Ralston's study. However, it should be pointed out that temperature appears to have negligible influence on polymer adsorption in our work. It is believed that this is most possibly due to the detection limit of anthrone method we used to measure HPGG concentration in solutions. The adsorption densities are rather low and there is great chance that any small changes of the density may not be detectable with anthrone method. Preliminary calculation shows that an error of 0.004 in the absorbance measurement of supernatant leads to a 0.005 mg/m^2 fluctuation in adsorption density data.

A polydisperse polymer has a more round adsorption isotherm than a monodisperse one (Roefs, Scheutjens et al. 1994). With an increasing degree of polydispersity the adsorption isotherms become more rounded because the shorter chains are progressively replaced by longer ones as the polymer concentration is

increased. Shorter chains are preferentially adsorbed due to the quick diffusion onto the interface at the beginning stage of adsorption. However, those pre-adsorbed shorter chains are gradually replaced by the longer chains due to the higher affinity of longer chains for the saturated surface (Jiang, Liu et al. 1998). Although exact polydispersity ratio of HPGG used in this work is not available as of this moment, it is widely accepted that natural polysaccharides are polydisperse polymers if no special separation processes were undertaken. Thus, the round shape and weak affinity type adsorption isotherms in this work are attributed to the polydispersity of HPGG. In addition, the presence of random physical entanglements of HPGG chains is also believed to able to increases the polymer polydispersity to some extent.

Pawlik and Laskowski concluded from their results that the amount of guar adsorbed on illite, which is around 0.20 mg/m^2, was independent of ionic strength over a wide range of salt concentrations (Pawlik and Laskowski 2006). In our study, not only HPGG adsorption at solid-liquid interface is studied but also HPGG/Borate adsorption on negatively charged hydrophobic surface in aqueous system. The specific complexation of borates with diols increases the negative charge of the HPGG and converts nonionic polysaccharide into an anionic polyelectrolyte. And due to the presence of negative charge on the polymer chain and thus the electrostatic repulse between HPGG and PSL-A, the maximum adsorption density of HPGG/Borate is reduced to 0.07 mg/m^2 from 0.12 mg/m^2 for adsorption of HPGG alone in the same conditions. Furthermore, the electrostatic repulsion between HPGG/Borate polymer chains adsorbed on the surface and that in solution can prevent

this negatively charged polymer from adsorbing to the surface any further. All these lead to a lower surface coverage with the introduction of borax. Adsorption behavior of HPGG/MBA was studied as well and shown in Figure 3-4. In comparison to Figure 3-3, the only difference involves the maximum adsorption density. HPGG/MBA maximum adsorption density on PSL-A was found to be around 0.06 mg/m^2, which is slightly smaller than that of HPGG/Borate adsorption.

With the addition of electrolyte into the suspension, the electrostatic interactions between the polymers and the particles are shielded. As expected the adsorption density in suspensions with sodium chloride concentrations of 0.10M is increased by about 0.03mg/m^2 compared to the suspensions with sodium chloride concentrations of 0.03M. Wang et al. (Wang, Somasundaran et al. 2005) pointed out that when hydrophobic force made a significant contribution to adsorption of a polymer on a mineral, the adsorption density would increase with the addition of salt due to "salting-out" effect. Water activity (solvent "goodness") can be reduced simply by the addition of an electrolyte that binds water in competition with the polymer. Such an increase was obtained in our work. Thus this may prove again that the hydrophobic force is the main driving force for the adsorption of HPGG on anionic polystyrene particle surface. However, it should be mentioned that one of the unique properties of guar and guar derivative solutions is "salt tolerance", which means guar-based polymers are soluble in salt solutions that contain up to 70% (by mass) monovalent cation salts (Pawlik and Laskowski 2006).

The experiment results from Jenkins and Ralson (Jenkins and Ralston 1998)

support the hypothesis that the mannose backbone of the guar chain adsorbs to the talc surface, leaving the pendant galactose groups protruding into the bulk solution. In our study hydroxypropyl substitution degree appears to have negligible effect on HPGG adsorption. This is attributed to the hypothesis that hydrophobic interaction between guar and hydrophobic surface mainly arise from that of the guar mannose backbone with the surface. It is thus expected that hydroxypropylation will not have much influence on guar adsorption and our results agree with this well.

Since guar and its derivatives contain a multiplicity of hydroxyl groups, complex formation between borates or borate derivatives can occur with an increase in the viscosity or gel formation, with changes in other properties related to molecular size (Martin, Freitas et al. 2003; Bishop, Shahid et al. 2004). The cross-linking of different polymer chains results in gelation, forming a three-dimensional network of connected chains via the borate ion or sometimes parts of the same chain (Figure 4-8). In aqueous solution boric acid exists as a pH dependent equilibrium with the borate anion such that higher pH drives the reaction towards the formation of the borate. The complexation of guar with borate and even the cross-linking via borate binding are obviously pH dependent as well. With the increase of pH, more boron will then be bound to HPGG polymer chain and thus results in an increasing of the charge density of HPGG/Borate. Electrophoresis results (Figure 3-6) in this study show that electrophoretic mobility values decrease along with the increase of pH. As shown in the adsorption isotherms, the introduction of borax into the system reduces the adsorption density of HPGG on negatively charged surface. With less polymer

adsorbed on the surface and thus the thinner adsorbed polymer layers, the electrophoretic behaviors of polystyrene particles covered with HPGG/Borate lies in between. Its electrophoretic mobility values, at higher pH especially, are found to be more negative than particles covered with HPGG but greater than those of the bare particles. In addition, the charge on adsorbed HPGG/Borate polyelectrolyte provides a compensation for the surface charge shielded by HPGG alone. The borate complexation reaches equilibrium beyond certain pH values which results in the plateau in electrophoretic mobility curve shown in Figure 3-6. We herein attribute the electrophoresis results for HPGG/Borate and HPGG/MBA covered particles to the two reasons mentioned above. It is interesting to note that the change of electrophoretic behavior of those particles occurs close to the pH range where the pKa values of borax and methylboronic acid lie.

As shown in Figure 3-6, there is a difference about 0.5×10^{-8} m^2/Vs in the plateau values of electrophoretic mobility of polystyrene particles covered by HPGG/Borate and HPGG/MBA. We speculate this is most possibly due to the cross-linking induced by borax. With borax present in a basic solution, cross-linking occurs and gel is formed. The charge domains on the polymer chain are likely to be buried in this three-dimensional structure and particles covered by HPGG/Borate thus tend to behave more like the ones covered by non-ionic polymers. However, for particles covered by HPGG/MBA no cross-linking is involved. Thus more boron is expected to be bound onto the polymer chain and there is less chance that those charge domains can be buried inside the polymer layer. We also guess that since no

cross-linking occurs for HPGG/MBA there might remain more hydroxyl groups on the polymer chain that are available for binding with methylboronic acid under the same experimental conditions. Therefore, more methylboronic acid molecules were bound to the polymer chain making it more negatively charged (Cui, Pelton et al. in preparation). This explanation can be confirmed by the dynamic light scattering data shown in Table 3-1.

The average diameter of polystyrene bare particles used in this study is 840 nm. After the complete adsorption of HPGG, the hydrodynamic size of the particles is increased to about 1240 nm. According to Picout and his co-workers (Picout, Ross-Murphy et al. 2001), the gyration radius of guar with the similar molecular weight to HPGG used in our work is around 100 nm in conditions close to our work. Due to the presence of pendent galactose groups, the associative effect of guar molecules is reduced and HPGG behaves more like a rigid polymer. Thus it is quite possible that we obtained the adsorbed polymer layer which is sparse and has a thickness of around 100 nm (Simon, Picton et al. 2005). According to our adsorption isotherm data and the estimated adsorption thickness, we calculated the HPGG concentration in the adsorbed polymer layer at the particles surfaces. The polymer concentration was found to be around 0.3g/L, which is about one third of the overlap concentration (c*) of HPGG. Therefore the adsorbed layer can be viewed as a sparse layer in our work. The diameter size of particles covered with HPGG/Borate is around 1140 nm. The thinner polymer layer can be explained by the less amount of HPGG adsorbed on particle surface. In addition, the presence of cross-linking for

HPGG/Borate is likely to compress the polymer layer and thus reduce the layer thickness. The adsorbed polymer layer for HPGG/MBA, on the other hand, is rather thicker but sparse. With no compression induced by borax cross-linking, the adsorbed HPGG/MBA layer is less dense, leading to a smaller adsorption density compared to HPGG/Borate. In addition, according to our hypothesis that more MBA might be bound to the polymer, the electrostatic repulsion between adsorbed polymer chains on the surface tend to cause the polymer layer sparser and thus thicker.

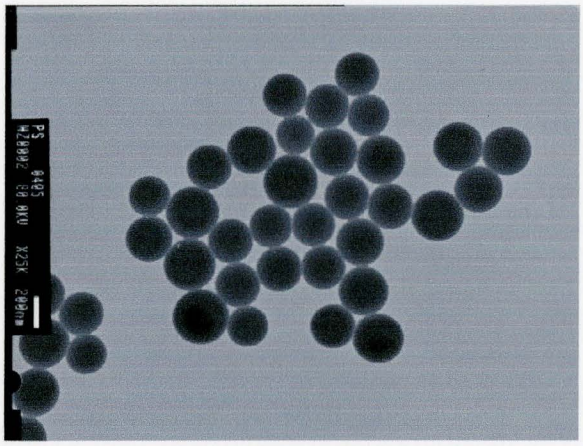

Figure 3-1 TEM image of cationic polystyrene particles (PSL-C).

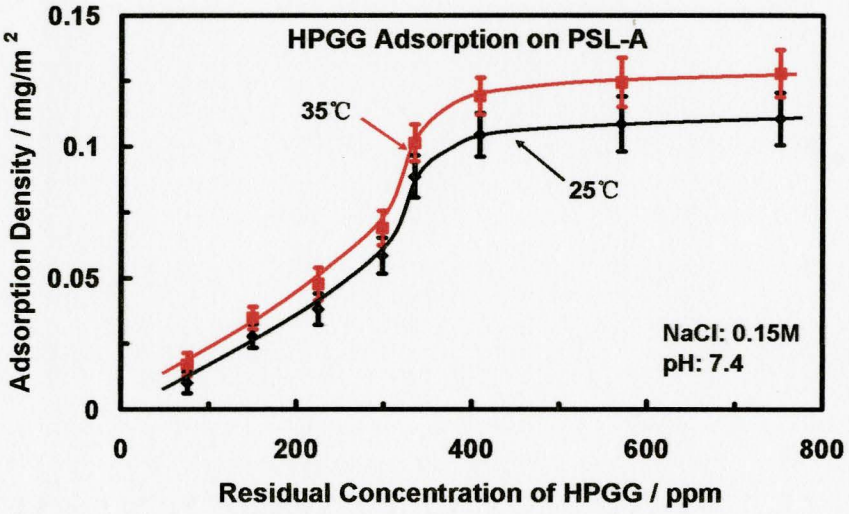

Figure 3-2 Adsorption isotherm for HPGG on anionic polystyrene latex (PSL-A) at pH 7.4 with a sodium chloride concentration of 0.15M (25 ℃ & 35 ℃; ppm: wt/wt).

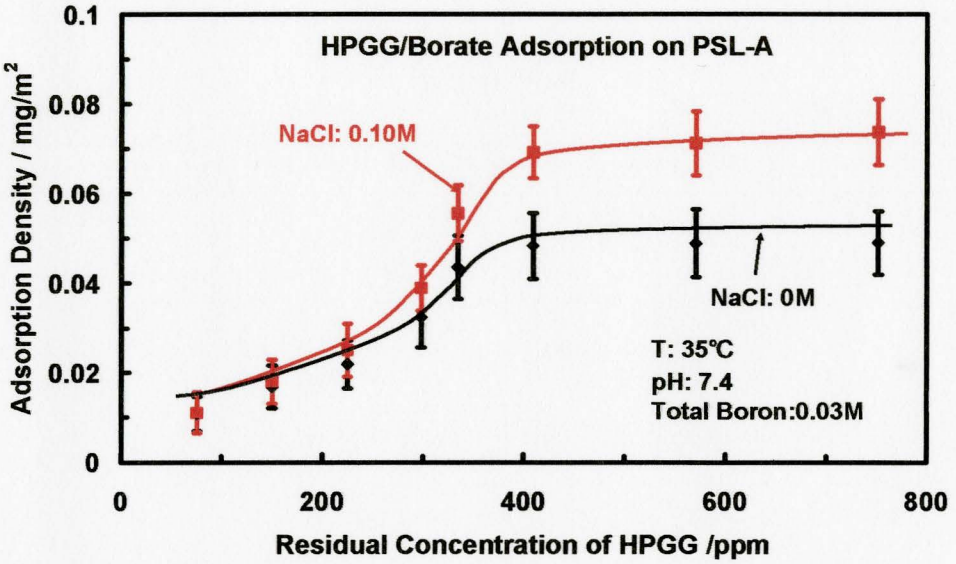

Figure 3-3 Adsorption isotherm of HPGG/borate on PSL-A at pH 7.4 and 35 ℃ (with sodium chloride concentrations of either 0.10M or 0M).

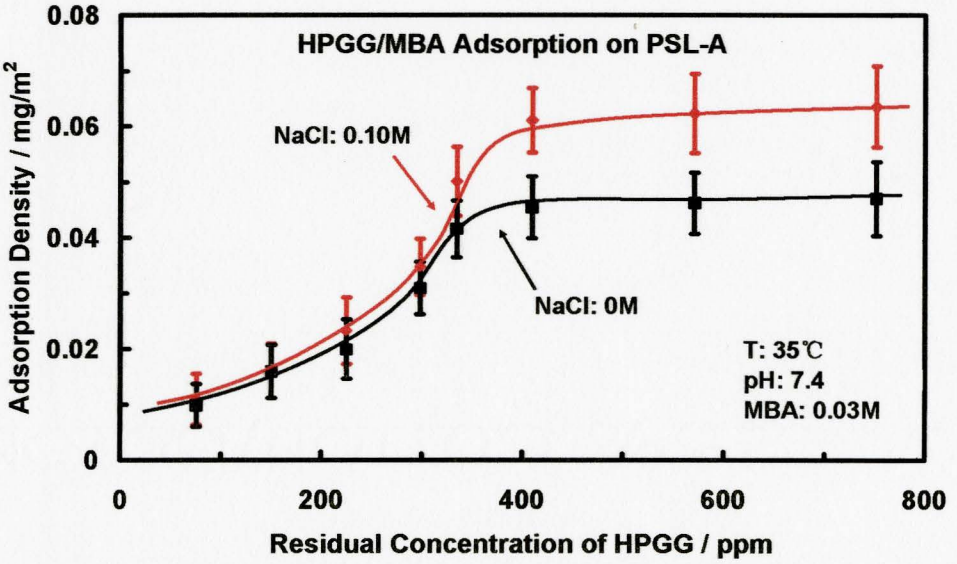

Figure 3-4 Adsorption isotherm of HPGG/MBA on PSL-A at pH 7.4 and 35 ℃ (with sodium chloride concentrations of either 0.10M or 0M; MBA: methylboronic acid).

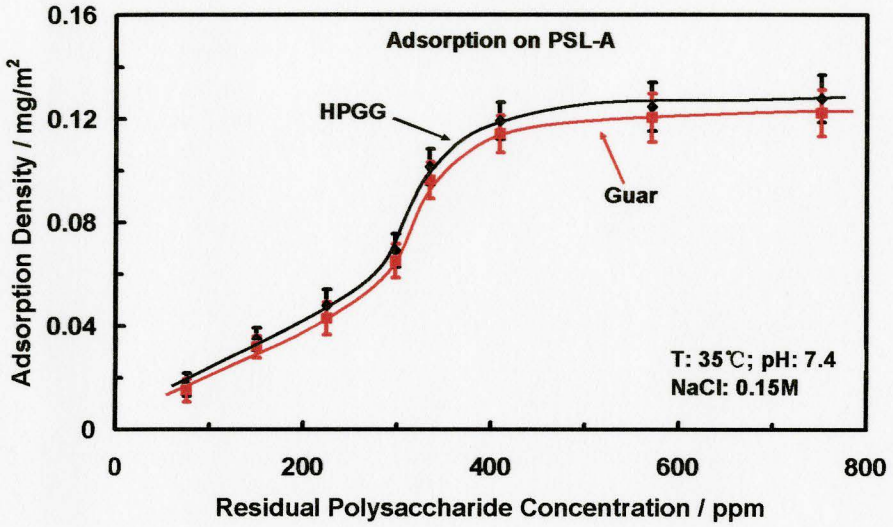

Figure 3-5 Adsorption isotherm of HPGG and guar on PSL-A at pH 7.4 and 35 ℃ with a sodium chloride concentration of 0.15M.

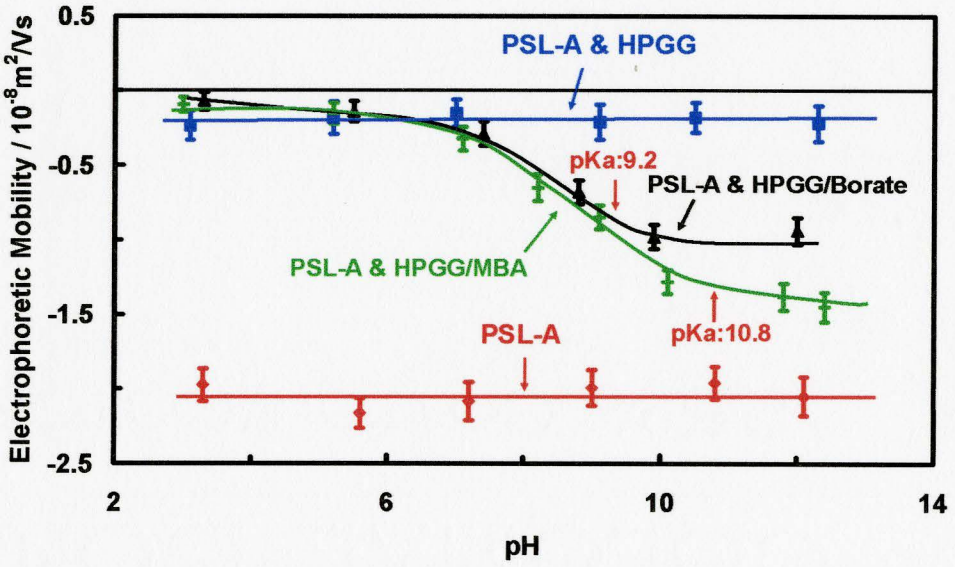

Figure 3-6 Electrophoretic mobility of PSL-A, PSL-A & HPGG, PSL-A & HPGG/Borax, and PSL-A & HPGG/MBA as a function of pH.

Chapter 4 Flocculation

The objective of this chapter is to present the flocculation behavior of latex HPGG mixtures in the presence of either borax or phenylboronic acid (PBA). In addition, the flocculation mechanisms are discussed in different cases. The redispersion of latex flocs with simple sugars is also reported.

4.1 Results

4.1.1 Calculation of polymer chain charge density

The concentrations of free and HPGG bound borate ions were calculated following the method described in our previous work, which involves the simultaneous solution of eq 1,2 in Figure 4-1 and the borate dissociation equilibrium. For experiments with added fructose, boron binding to diols on monosaccharide sugar rings after addition of D- Fructose were described by eq 3 in Figure 4-1. The calculation of charge density on HPGG/Borate chain required the concentration of boron binding sites, which is a function of the HPGG concentration, the degree of hydroxypropylation, and the galactose concentration. Our assumptions are that all hydroxyl groups had the same probability of hydroxypropyl substitution and boron reacts only with galactose. The mass concentration of HPGG was then converted to a molar concentration of boron binding sites. K_3 as Figure 4-1 was chosen to be 1698 L/mol at 298 K according to Vandenberg (Vandenberg, Peters et al. 1994). The charge density was defined as the ratio of the concentration of HPGG bound boron over the

total HPGG binding site concentration. The three equilibrium equations were solved using the MathCAD 12 solver with the TOL set to 10^{-12}.

4.1.2 Flocculation and Redispersion

The residual turbidities of HPGG solutions alone and in the presence of either borax or phenylboronic acid (PBA) after the addition of cationic polystyrene particles (PSL-C) were measured as a function of HPGG concentration and the results are summarized in Figure 4-2. It is found that the supernatant turbidity of the samples with borax decreased first with HPGG concentration over the range of 3 orders of magnitude and then increased again. Measurements were also obtained for samples with PBA and the results showed that supernatant turbidity decreased first and beyond certain HPGG concentration it started to decrease. In comparison to flocculation induced by HPGG/Borate, the flocculation induced by HPGG/PBA shows narrower flocculation range. And for the suspensions with no boron, there was nearly no change of the turbidity with the increase of HPGG concentration and thus no distinct flocculation induced solely by HPGG were observed.

The electrophoretic mobility values of HPGG alone and in the presence of either borax or PBA (pKa=8.8) after the addition of PSL-C were measured as a function of HPGG concentration (Figure 4-3). As the HPGG concentration was increased, electrophoretic mobility values for suspensions added with either borax or PBA groups both decreased from positive to negative and then leveled off beyond certain HPGG concentrations. The plateau values of electrophoretic mobility are

around -1.0×10^{-8} m^2/Vs and -2.0×10^{-8} m^2/Vs for suspensions added with borax and PBA, respectively. A decrease of electrophoretic mobility values from around 2.5×10^{-8} m^2/Vs to 0.3×10^{-8} m^2/Vs was also observed for the suspensions in the absence of borate but no charge reversal was found in our work. For comparison, electrophoretic mobility of PSL-C in the absence of HPGG was also investigated. As shown in Figure 4-6, with borate dissolved in the positively charged polystyrene suspension, electrophoretic mobility was found to decrease slowly with the increase of pH. However, no charge reversal was found in the measurements.

To study pH effect on HPGG/Borate flocculation efficiency, residual turbidity and electrophoretic mobility of the suspensions were investigated and the results are plotted in Figure 4-4. As the pH values were reduced from 11.1 to 6.5, it was obtained that residual turbidity of the supernatant increased and floccs formed previously due to the introduction of HPGG/Borate to cationic polystyrene latex particles were redispersed into water again. Electrophoretic mobility curve in Figure 4-3 also displays the same behavior along with the reduction of pH as turbidity.

In Figure 4-5-a, the residual turbidity and electrophoretic mobility data were plotted as functions of the HPGG/Borate chain charge density that were calculated using the method mentioned previously. By adding D-Fructose to the mixture with optimum flocculation, the diols on monosaccharide sugar rings will compete against HPGG for boron and thus the charge density on HPGG/Borate chain was reduced. Floccs settled down at the bottom of flask then redissolved again within 30 min gentle stirring, leading to the increase of residual turbidity as measured in this work.

Electrophoretic mobility was also found to increase from negative values to rather neutral if charged density was decreased by simply adding increasing amount of D-Fructose (Figure 4-5-a).

4.2 Discussion

When only HPGG is present in the suspension of cationic polystyrene particles, no specific influence on particle stability was obtained as shown in Figure 4-2. However, preliminary experiments show that HPGG alone can flocculate PSL-C to some extent over a rather narrow concentration range (Figure 4-2-b). The reason why flocculation was not obtained in Figure 4-2-a is that the HPGG concentrations stand far from each other so we actually missed the points where effective flocculation occurs. Singh et al. also found that HPGG and its derivative grafted with polyacrylamide were able to flocculate kaolin, iron ore, and silica suspensions (Nayak and Singh 2001).

Though it was obtained that both HPGG/Borate and HPGG/PBA could lead to the flocculation of positively charged particles as shown in Figure 4-2-a, HPGG/Borate was found to be able to flocculate PSL-C over a broader HPGG concentration range than that of HPGG/PBA. And thus the flocculation mechanisms in two systems are expected to be different.

In the case of HPGG/PBA, the non-ionic polymer was converted to negatively charged polyelectrolyte due to the binding of PBA on the polymer chain. HPGG/PBA behaves like a labile polyelectrolyte and rigid polymer because of the

electrostatic repulsion between neighboring PBA bound on the polymer chain. Due to the electrostatic attraction between this newly formed polyelectrolyte and the residual charge groups on the particle surfaces, segments of the polyelectrolyte were adsorbed onto the particle surfaces and those un-adsorbed segments were left protruding into the bulk solution. And those protruding trains and tails were still likely to attach the bare areas on the surface of neighboring particles and bridge them together. Bridging flocculation is thus employed here to explain the flocculation behavior of HPGG/PBA. Generally speaking, flocculants are most effective at adsorption densities corresponding only to a fraction of the complete surface coverage, around 50% in most cases. This is confirmed by the residual turbidity results (Figure 4-2-a) that show that PSL-C flocculation is most pronounced at intermediate HPGG concentrations. At higher polymer adsorption densities, electrosteric stabilization takes place and leads to redispersion of the cationic particles. This process is commonly classified as bridging flocculation (Figure 4-7). As more HPGG is added to the solution, more polymers will be adsorbed onto the particle surfaces until the saturation is reached. When the surface is totally covered with HPGG, the particles are re-stabilized with the polymer acting as steric stabilizer and the flocculation will re-disperse into water again as shown in Figure 4-2-a.

Whereas in the case of HPGG/Borate, we believe some more complicated flocculation mechanism was involved considering the broader flocculation range. The HPGG polymer chains will be cross-linked into three dimensional networks with the addition of borax under basic conditions. Unlike those single HPGG polymer chains

bound with PBA, HPGG/Borate can be viewed as the polyelectrolyte with increasing molecular weight due to the presence of cross-linking. As shown in Schwarz's works (Schwarz, Bratskaya et al. 2006; Schwarz, Jaeger et al. 2007), polymers with higher molecular weight show much broader flocculation range. When polymer concentrations are really small and effective flocculation is not possible for polymers with lower molecular weight, the polymers with high molecular weight are found to be able to flocculate the particles rather well. Similar to the results in Schwarz's works, effective flocculation was also obtained in our study when HPGG concentration is low. As the HPGG are tuned to the cross-linked polyelectrolyte with huge molecular weight, a single one of the newly formed polymer networks is believed to be able to adsorb more oppositely charge particles and bridge them together. Therefore, lower polymer concentrations are required to induce the flocculation for HPGG/Borate. As the HPGG concentration is increased to the point where HPGG/PBA was able to stabilize PSL-C, effected flocculation was still obtained for HPGG/Borate. This is believed to be due to the different conformation of adsorbed HPGG on the surfaces of particles. With HPGG/PBA, the adsorbed polyelectrolyte is expected to assume a thinner and flatter polymer layer conformation. But with HPGG/Borate, the adsorbed polymer is more likely a thick polymer network and more polymers are required to cover the particle surfaces completely to re-stabilize them.

In addition, with the total boron concentration remaining the same in all flocculation experiments but increasingly added HPGG, the HPGG polymer chains

will compete with each other for boron in the solution. Thus, the possibility of cross-linking is smaller and the HPGG/Borate polymer molecular weight is expected to be reduced compared to dilute polymer solutions. In the presence of mechanical shearing stress during stirring in flocculation experiments, we believe a process of de-cross-linking and de-networking occurs at higher polymer concentrations. Considering the fact that HPGG-Borate binding is labile, we think floccs induced by HPGG/Borate networks are likely to break down with mechanical strength. And the HPGG/Borate adsorbed on the particles surfaces will be likely to change the conformation when the de-cross-linked boron binds to the hydroxyl groups in the same HPGG/borate network instead of the neighboring polymer networks. With the conformation change and more polymer adsorption on the surface, the particles will be completely covered with the polymer. Therefore, flocculation disappears at higher polymer concentrations and PSL-C is stabilized again. This explains well why flocculation can be achieved over a rather broad range of polymer dosages. And therefore we suggest that the flocculation induced by HPGG/borate in this study is a synergic effect of bridging flocculation and network flocculation (Figure 4-8). We believe that network flocculation is the major flocculation mechanism occurred in the study of HPGG/Borate.

Borate and phenylboronic acid binding to adsorbed HPGG on particle surface are reflected as well in our electrophoresis results (Figure 4-3). When no boron is present and only HPGG is adsorbed on the surface, the electrophoretic mobility values of the particles covered with HPGG alone decrease from $+2.4\times10^{-8}\,m^2/Vs$ to

0.3 $\times 10^{-8}$ m^2/Vs along with the increasing polymer concentrations in solution. This can be explained by the fact that with more HPGG available for adsorption in the bulk solution more HPGG is likely to adsorb onto the surface until a maximum adsorption density is reached. And as the nonionic HPGG adsorbs onto particles surfaces, the polymer layer then pushes shear plane far away from the surface, decreasing the electrophoretic mobility. As shown in Figure 4-3 for HPGG/Borate, with the increase of HPGG concentration in solution and thus the adsorbed HPGG/Borate on particles surfaces, electrophoretic mobility values decrease from $+2.4\times10^{-8}$ m^2/Vs for bare particles to -1.1×10^{-8} m^2/Vs for fully covered particles. The charge reversal in this study is simply due to the introduction of borax. The presence of negatively charged HPGG/Borate layer adsorbed onto the positively charged surface is attributed to the surface charge reversal as shown in the electrophoresis results. This negatively charged polymer layer on the surface not only works as a barrier shielding the positive charge of the particle but also provides negative charge to the newly formed soft particle.

Though similar electrophoretic properties were obtained with HPGG/PBA, the electrophoretic mobility values for fully covered particles with PBA bound HPGG appear more negative with a plateau value around $-2.0\times10^{-8}$$m^2$/Vs. We suggest that for the borax, borate anions are more likely to be buried in the gels formed by cross-linking; for the phenylboronic acid, the anions are more exposed at the surfaces of adsorbed layer instead of the inside of three dimensional structure. In addition, without cross-linking taking up the hydroxyl groups on the polymer chain, more

phenylboronic acid molecules are expected to be bound to the chain. Thus, the charge density of HPGG/PBA is increased compared to that of HPGG/Borate, which eventually results in the more negative electrophoretic mobility values (Cui, Pelton et al. in preparation).

Considering the pH dependence of borax complexation with HPGG, pH influence on HPGG/Borate flocculation was studied by measuring residual turbidity of the suspensions with varied pH values. Figure 4-4 shows that the residual turbidity was reduced with the increasing pH, which means flocculation extent is greater at higher pH values. When pH value is high, especially above the pKa value of borax, HPGG is charged to some extent and thus works as an effective flocculant as shown in Figure 4-4. It should be pointed out that borax binding with HPGG is a labile interaction and with reduced pH the boron can be de-attached from the HPGG polymer chain. The results illustrated in Figure 4-4 agree with this well. At lower pH the residual turbidity increase which means floccs are redispersed into the solvent again and the flocculation of positively charged particles with HPGG/Borate is poor in this condition. Without the binding of borax onto the polymer chain, the non-ionic HPGG was obtained to be not able to flocculate cationic colloid. This is also confirmed by electrophoresis results shown in Figure 4-4. And an interesting resemblance of the shape of electrophoretic mobility curve and residual turbidity curve was found in this figure. We believe that the proposed interpretation agrees well with our results.

To exclude the effect of borax adsorption on particles on electrophoresis

results, electrophoretic mobility values of PSL-C in the absence of HPGG were measured and illustrated in Figure 4-6. It was obtained that the cationic colloids remained positively charged through the whole pH range. The decreasing of mobility values with the increase of pH is attributed to the salt effect of borax.

Not only does pH have an influence on borax binding to HPGG, but also monosaccharide added to the mixture has an effect on the borax binding equilibrium. Residual turbidity and electrophoretic mobility were plotted in Figure 4-5-a against the charged density of HPGG/Borate polymer chain. It is obtained that the charge density of polymer chain has a direct influence on the flocculation behavior of HPGG/Borate. With D- Fructose added to the flocculation and competing against HPGG for borate, originally bound borate to HPGG would come off from the polymer chain and reduce the charge density of this labile polyelectrolyte. This results in the redispersion of flocculation, turbidity increase and electrophoretic mobility turning more positive (Figure 4-5-a). Again, the shape of residual turbidity curve resembles with that of the electrophoretic mobility as shown in Figure 4-5-a. Within the polymer concentration range studied in this study, polymers with higher charge density were demonstrated to be the more effective flocculants. The reason why flocculation properties of polymers with even higher charge density were not investigated is that there involves an equilibrium for monosaccharide competing for borate against HPGG and only charge density below some certain value can be achieved according to our calculation.

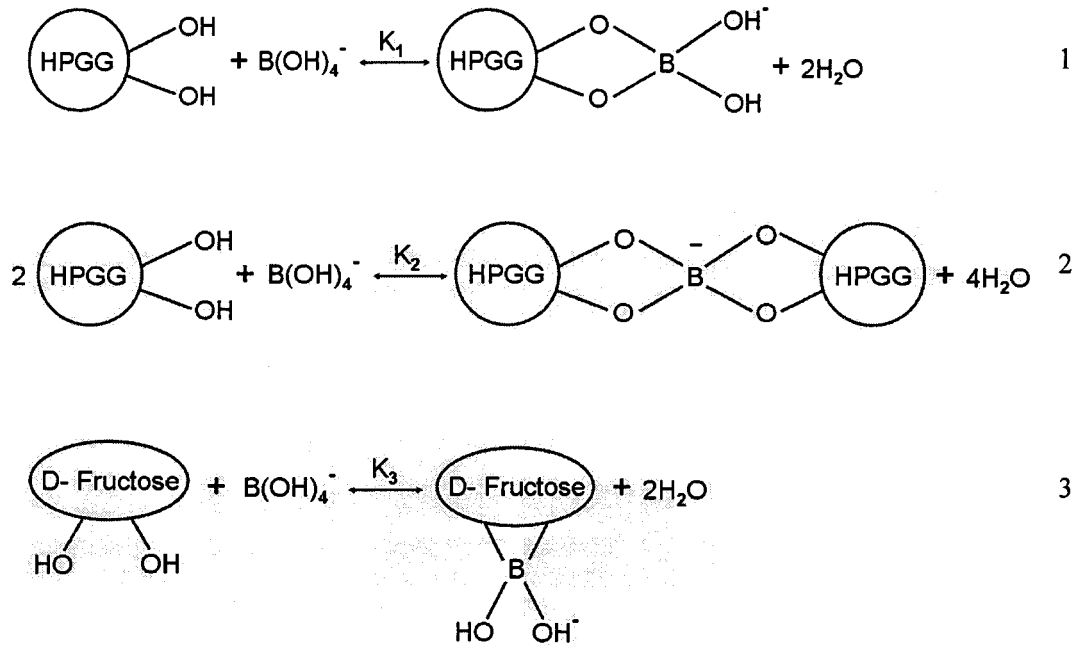

Figure 4-1 Schematic illustration of borate binding with borate and D-Fructose.

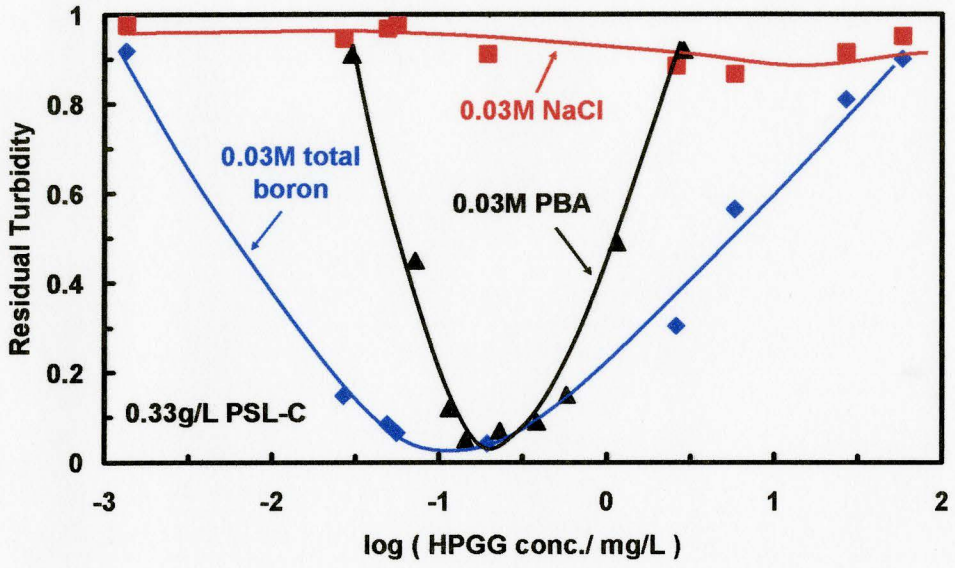

(a)

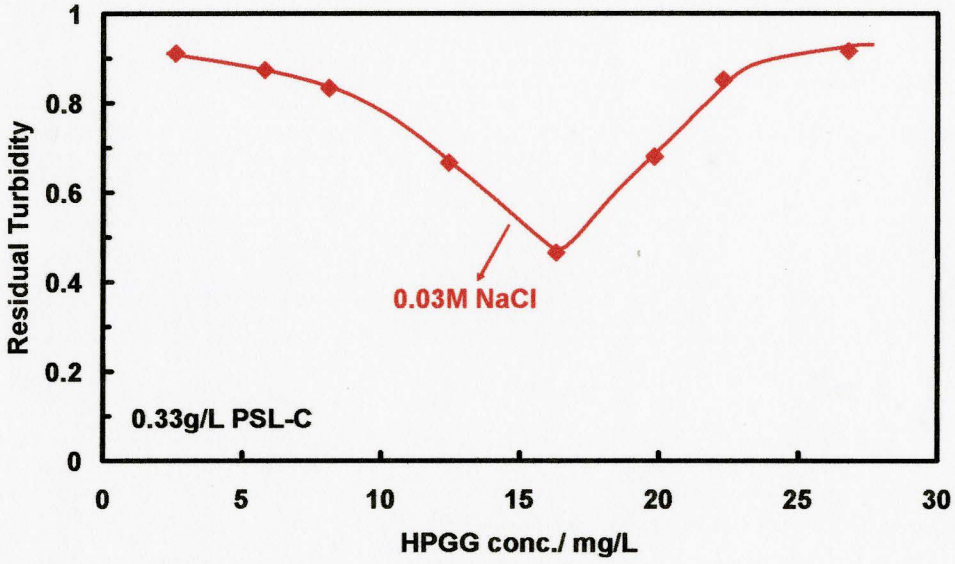

(b)

Figure 4-2 a: Residual turbidity measured at pH 9.0 using UV/Vis Spectrophotometer as a function of HPGG concentration for polystyrene latex, polystyrene latex added with borax (labeled "total boron") and polystyrene latex added with phenylboronic acid (labeled "PBA"); b: Residual turbidity measured using UV/Vis Spectrophotometer as a function of HPGG concentration for polystyrene latex only.

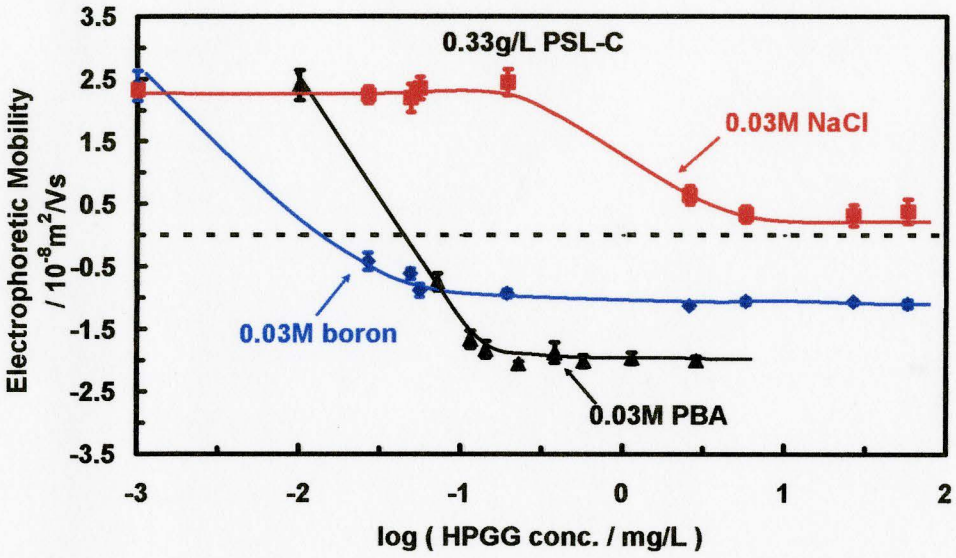

Figure 4-3 Electrophoretic mobility of polystyrene latex, polystyrene latex added with borax and polystyrene latex added with phenylboronic acid as a function of logarithm values of HPGG concentration.

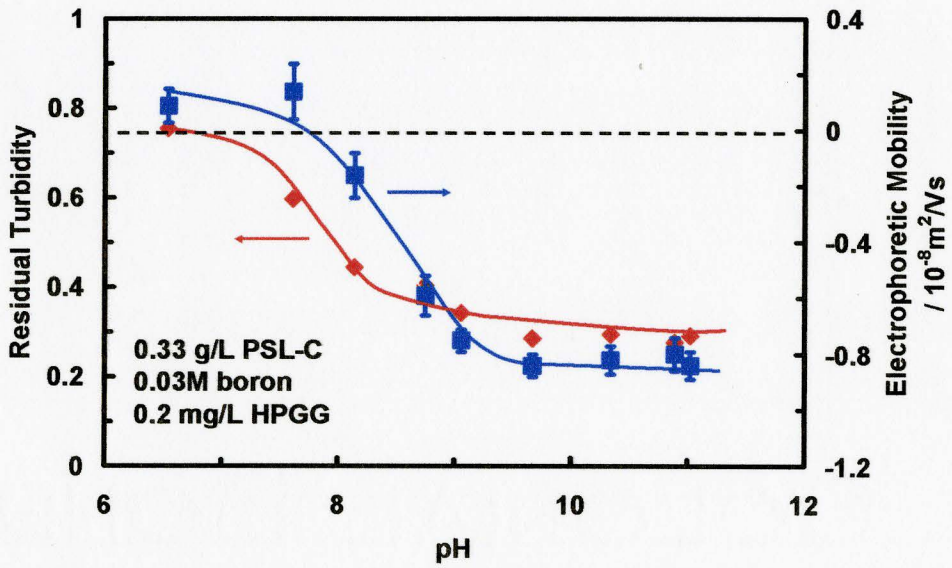

Figure 4-4 Residual turbidity and electrophoretic mobility of flocculation of positively charged particles with HPGG/Borate as a function of pH.

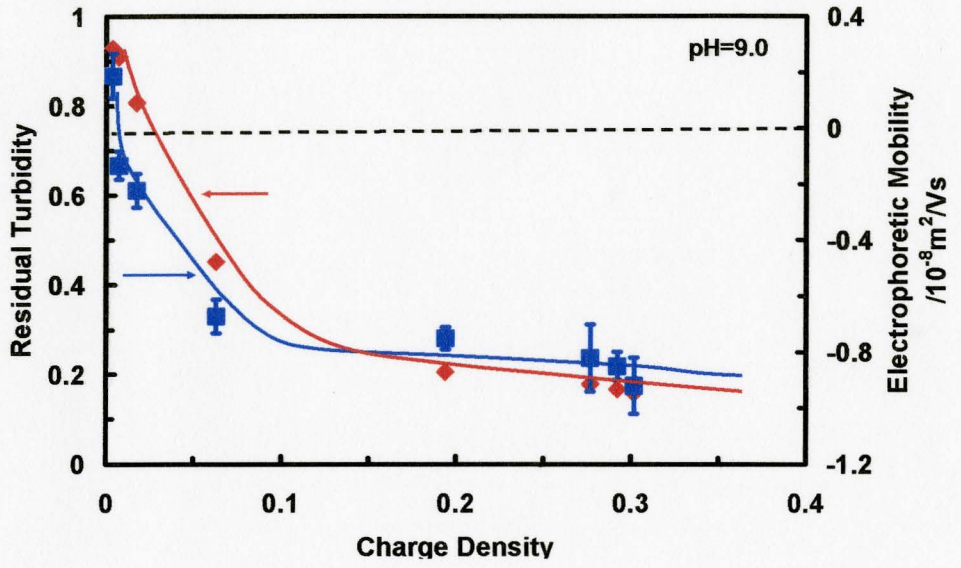

(a)

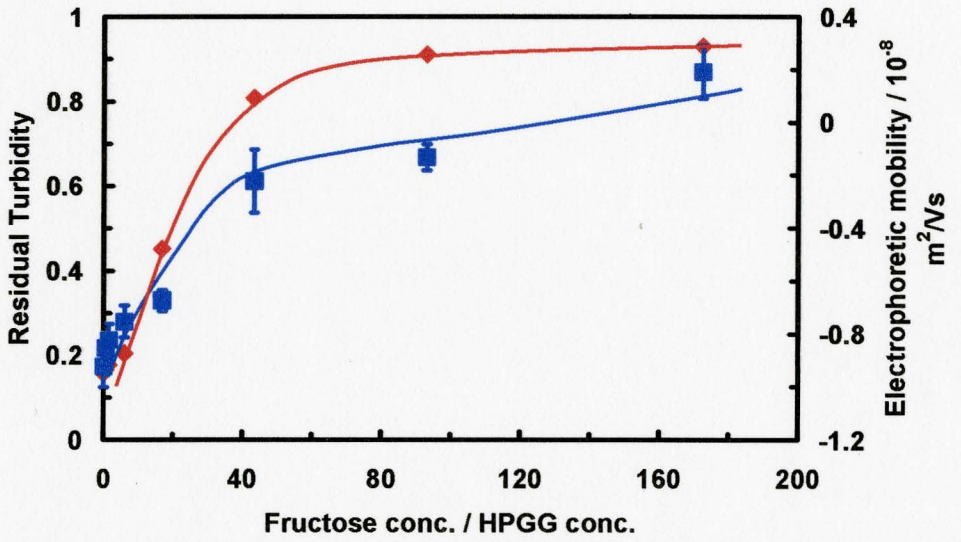

(b)

Figure 4-5 Residual turbidity and electrophoretic mobility of flocculation of positively charged particles with HPGG/Borate as a function of polymer chain charge density (a) and ratio of fructose concentrations over HPGG concentrations (b) on HPGG/Borate. HPGG concentration: 206.8mg/L.

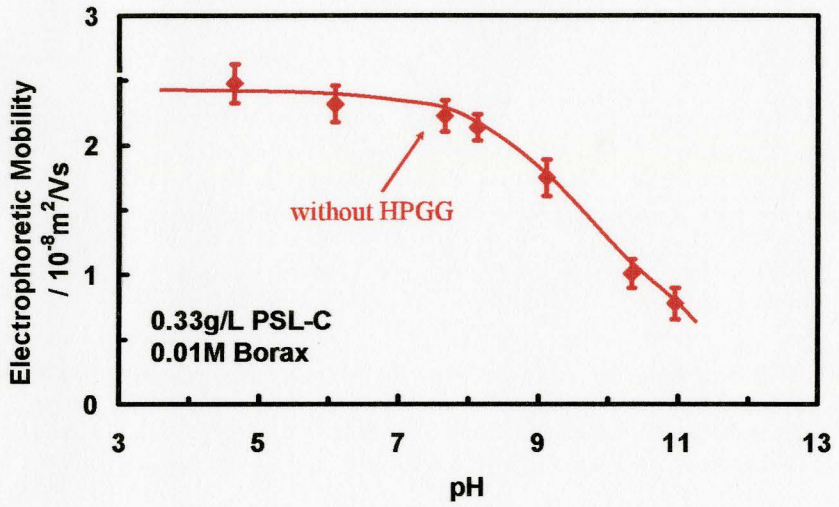

Figure 4-6 Electrophoretic mobility of cationic polystyrene latex in the absence of HPGG as a function of pH (added with 0.01M borax buffer).

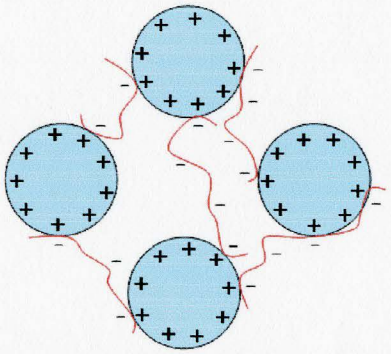

Figure 4-7 Proposed flocculation mechanism of cationic polystyrene latex with HPGG/Phenylboronic acid.

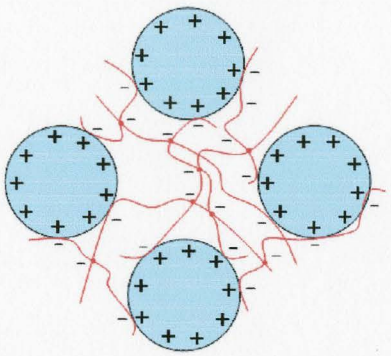

Figure 4-8 Proposed flocculation mechanism of cationic polystyrene latex with HPGG/Borax.

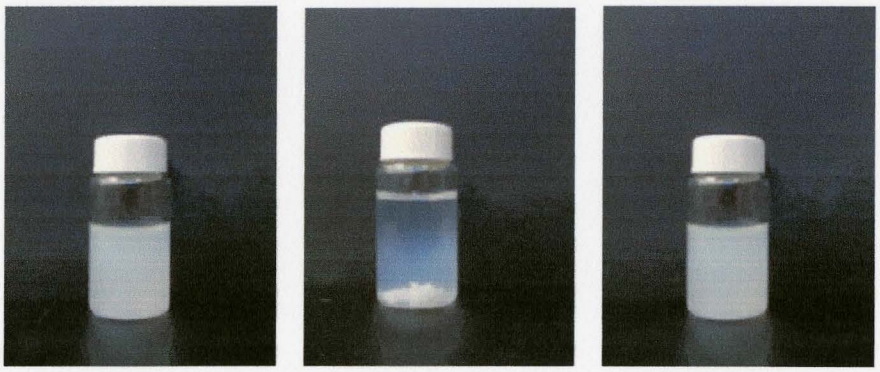

Figure 4-9 Pictures of cationic polystyrene latex before flocculation (left), after flocculation (middle), and after redispersion (right).

Chapter 5 Conclusions and Recommendations

The goal of this research was to try to investigate the properties of HPGG and borate bound HPGG at the solid-liquid interfaces. Polystyrene particles were employed in this study as the model hydrophobic surfaces at the tear film-corneal epithelium interfaces. The adsorption of HPGG on anionic and cationic particle surfaces was studied and the results obtained are expected to be helpful for future researchers in understanding of HPGG effect on tear film stability. What is more interesting is that HPGG bound with borate was found be an effective flocculant for cationic colloid. Not only does this finding help us improve the understanding of flocculation mechanism present in many industry applications but also it might have some impacts on the flocculant industry.

Conclusions:

(1) HPGG adsorption on anionic polystyrene particles leads to thick but sparse layers and this adsorption is characterized as a weak-affinity adsorption. The adsorption forces are suggested to arise from hydrophobic interactions between HPGG backbone and particles.

(2) Addition of borate lowers the adsorption of HPGG onto anionic particles. This influence was found to be lessened by increasing ionic strength in the suspension for adsorption experiments.

(3) The degree of hydroxypropyl substitution was found to have negligible effect on HPGG adsorption on anionic particles.

(4) Borax and methylboronic acid binding to HPGG is reflected in the electrophoresis. Along with dynamic light scattering data, adsorbed polymer layers of HPGG/Borate and HPGG/Methylboronic acid are compared and the possible structure of adsorbed layer is proposed.

(5) HPGG bound with borate behaves as a labile polyelectrolyte and was demonstrated to be able to induce the flocculation of oppositely charged latexes.

(6) Through adjusting pH and adding fructose, the charge density of HPGG/Borate can be varied and it is found to be capable of flocculating cationic colloids.

(7) Positively charged latexes were flocculated by HPGG/Borate over a broad range of HPGG concentration, which is proposed to be a result of network flocculation and bridging flocculation under our experimental conditions.

(8) Flocculation induced by HPGG/Phenylboronic acid on the other hand shows narrower flocculation range, which is proposed to be due to the absence of borate cross-linking and only bridging flocculation works.

The following aspects are recommended for any future studies:

(1) It would be interesting to explore the structure of adsorbed polymer layer on the surface and the conformational change of this layer thereafter.

(2) The mucin adsorption on hydrophobic surfaces needs to be investigated and compared to the adsorption of HPGG.

(3) The binding constant of borate with HPGG is an important parameter in our study and it would be truly helpful if this could be measured successfully through some experimental approaches.

References

Adachi, Y. (1995). "Dynamic Aspects of Coagulation and Flocculation." Advances in Colloid and Interface Science **56**: 1-31.

Bassil, E., H. N. Hu, et al. (2004). "Use of phenylboronic acids to investigate boron function in plants. possible role of boron in transvacuolar cytoplasmic strands and cell-to-wall adhesion." Plant Physiology **136**(2): 3383-3395.

Bishop, M., N. Shahid, et al. (2004). "Determination of the mode and efficacy of the cross-linking of guar by borate using MAS B-11 NMR of borate cross-linked guar in combination with solution B-11 NMR of model systems." Dalton Transactions(17): 2621-2634.

Blakeney, A. B. and L. L. Mutton (1980). "A Simple Colorimetric Method for the Determination of Sugars in Fruit and Vegetables." Journal of the Science of Food and Agriculture **31**(9): 889-897.

Bratskaya, S., V. Avramenko, et al. (2006). "Enhanced flocculation of oil-in-water emulsions by hydrophobically modified chitosan derivatives." Colloids and Surfaces a-Physicochemical and Engineering Aspects **275**(1-3): 168-176.

Carnali, J. O. (1992). "Gelation in Physically Associating Biopolymer Systems." Rheologica Acta **31**(5): 399-412.

Chen, C. Y., J. Y. Guo, et al. (1998). "Dynamic light scattering of dilute PVA-borax aqueous solutions." Journal of Polymer Research-Taiwan **5**(2): 67-76.

Cheng, Y., K. M. Brown, et al. (2002). "Characterization and intermolecular interactions of hydroxypropyl guar solutions." Biomacromolecules **3**(3): 456-461.

Christensen, M. T., S. Cohen, et al. (2004). "Clinical evaluation of an HP-guar gellable lubricant eye drop for the relief of dryness of the eye." Current Eye Research **28**(1): 55-62.

Goodwin, J. W., R. H. Ottewill, et al. (1979). "Studies on the preparation and

characterization of monodisperse polystyrene latices V.: The preparation of cationic latices." Colloid & Polymer Science **257**(1): 61-69.

Holly, F. J. (1987). "Tear Film Physiology." International Ophthalmology Clinics **27**(1): 2-6.

Holly, F. J. (1993). "Diagnostic Methods and Treatment Modalities of Dry Eye Conditions." International Ophthalmology **17**(3): 113-125.

Israels, R., J. Scheutjens, et al. (1993). "Adsorption of Ionic Block-Copolymers - Self-Consistent-Field Analysis and Scaling Predictions." Macromolecules **26**(20): 5405-5413.

Jasinski, R., D. Redwine, et al. (1996). "Boron equilibria with high molecular weight guar: An NMR study." Journal of Polymer Science Part B-Polymer Physics **34**(8): 1477-1488.

Jeffrey, G. C. and R. H. Ottewill (1988). "Reversible aggregation Part I. Reversible flocculation monitored by turbidity measurements." Colloid & Polymer Science **266**(2): 173-179.

Jenkins, P. and J. Ralston (1998). "The adsorption of a polysaccharide at the talc aqueous solution interface." Colloids and Surfaces a-Physicochemical and Engineering Aspects **139**(1): 27-40.

Jiang, J. W., H. L. Liu, et al. (1998). "Lattice Monte Carlo simulation of polymer adsorption at an interface, 2 - Polydisperse polymer." Macromolecular Theory and Simulations **7**(1): 113-117.

Johnson, M. E., P. J. Murphy, et al. (2006). "Effectiveness of sodium hyaluronate eyedrops in the treatment of dry eye." Graefes Archive for Clinical and Experimental Ophthalmology **244**(1): 109-112.

Kesavan, S. and R. K. Prudhomme (1992). "Rheology of Guar and Hpg Cross-Linked by Borate." Macromolecules **25**(7): 2026-2032.

Laskowski, J. S., Q. Liu, et al. (2007). "Current understanding of the mechanism of

polysaccharide adsorption at the mineral/aqueous solution interface." International Journal of Mineral Processing **84**(1-4): 59-68.

Liu, G. S., Q. M. Feng, et al. (2006). "Adsorption of polysaccharide onto talc." Minerals Engineering **19**(2): 147-153.

Lu, C., L. Kostanski, et al. (2005). "Hydroxypropyl guar-borate interactions with tear film mucin and lysozyme." Langmuir **21**(22): 10032-10037.

Lu, C. and R. Pelton (2001). "PEO flocculation of polystyrene-core poly(vinylphenol)-shell latex: An example of ideal bridging." Langmuir **17**(25): 7770-7776.

Ma, X. D. and M. Pawlik (2005). "Effect of alkali metal cations on adsorption of guar gum onto quartz." Journal of Colloid and Interface Science **289**(1): 48-55.

Mahammad, S., D. A. Comfort, et al. (2007). "Rheological properties of guar galactomannan solutions during hydrolysis with galactomannanase and alpha-galactosidase enzyme mixtures." Biomacromolecules **8**(3): 949-956.

Martin, S., R. A. Freitas, et al. (2003). "Physico-chemical aspects of galactoxyloglucan from the seeds of Hymenaea courbaril and its tetraborate complex." Carbohydrate Polymers **54**(3): 287-295.

Mer, V. K. L. and T. W. Healy (1963). THE ROLE OF FILTRATION IN INVESTIGATING FLOCCULATION AND REDISPERSION OF COLLOIDAL DISPERSIONS. **67:** 2417-2420.

Mitchell, J. R. and S. E. Hill (1995). "The Use and Control of Chemical-Reactions to Enhance the Functionality of Macromolecules in Heat-Processed Foods." Trends in Food Science & Technology **6**(7): 219-224.

Nayak, B. R. and R. P. Singh (2001). "Comparative studies on the flocculation characteristics of polyacrylamide grafted guar gum and hydroxypropyl guar gum." Polymer International **50**(8): 875-884.

Nijenhuis, K. T. (1997). Thermoreversible networks - Viscoelastic properties and

structure of gels - Introduction. Thermoreversible Networks. **130:** 1-12.

Paulsen, F. P. and M. S. Berry (2006). "Mucins and TFF peptides of the tear film and lacrimal apparatus." Progress in Histochemistry and Cytochemistry **41**(1): 1-53.

Pawlik, M. and J. S. Laskowski (2006). "Stabilization of mineral suspensions by guar gum in potash ore flotation systems." Canadian Journal of Chemical Engineering **84**(5): 532-538.

Pelton, R., B. Cabane, et al. (2007). "Shapes of polyelectrolyte titration curves. 1. Well-behaved strong polyelectrolytes." Analytical Chemistry **79**(21): 8114-8117.

Pezron, E., A. Ricard, et al. (1988). "Reversible Gel Formation Induced by Ion Complexation .1. Borax Galactomannan Interactions." Macromolecules **21**(4): 1121-1125.

Picout, D. R., S. B. Ross-Murphy, et al. (2001). "Pressure cell assisted solution characterization of polysaccharides. 1. Guar gum." Biomacromolecules **2**(4): 1301-1309.

Roefs, S., J. Scheutjens, et al. (1994). "Adsorption Theory for Polydisperse Polymers." Macromolecules **27**(17): 4810-4816.

Saffour, Z., P. Viallier, et al. (2006). "Rheology of gel-like materials in textile printing." Rheologica Acta **45**(4): 479-485.

Schwarz, S., S. Bratskaya, et al. (2006). "Effect of charge density, molecular weight, and hydrophobicity on polycations adsorption and flocculation of polystyrene latices and silica." Journal of Applied Polymer Science **101**(5): 3422-3429.

Schwarz, S., W. Jaeger, et al. (2007). "Cationic flocculants carrying hydrophobic functionalities: Applications for solid/liquid separation." Journal of Physical Chemistry B **111**(29): 8649-8654.

Simon, S., L. Picton, et al. (2005). "Adsorption of amphiphilic polysaccharides onto polystyrene latex particles." Polymer **46**(11): 3700-3707.

Singh, R. P., S. Pal, et al. (2006). "A high performance flocculating agent and viscosifiers based on cationic guar gum." Macromolecular Symposia **242**: 227-234.

Sinton, S. W. (1987). "Complexation Chemistry of Sodium-Borate with Polyvinyl-Alcohol) and Small Diols - a B-11 Nmr-Study." Macromolecules **20**(10): 2430-2441.

Srivastava, M. and V. P. Kapoor (2005). "Seed gallactomannans: An overview." Chemistry & Biodiversity **2**(3): 295-317.

Thomas, D. N., S. J. Judd, et al. (1999). "Flocculation modelling: A review." Water Research **33**(7): 1579-1592.

Ubels, J. L., D. P. Clousing, et al. (2004). "Pre-clinical investigation of the efficacy of an artificial tear solution containing hydroxypropyl-guar as a gelling agent." Current Eye Research **28**(6): 437-444.

Vandenberg, R., J. A. Peters, et al. (1994). "The Structure and (Local) Stability-Constants of Borate Esters of Monosacchharides and Disaccharides as Studied by B-11 and C-13 Nmr-Spectroscopy." Carbohydrate Research **253**: 1-12.

Viles, F. J. and L. Silverman (1949). Determination of Starch and Cellulose with Anthrone. **21:** 950-953.

Wang, J. and P. Somasundaran (2007). "Study of galactomannose interaction with solids using AFM, IR and allied techniques." Journal of Colloid and Interface Science **309**(2): 373-383.

Wang, J., P. Somasundaran, et al. (2005). "Adsorption mechanism of guar gum at solid-liquid interfaces." Minerals Engineering **18**(1): 77-81.

Xiao, H. N., R. Pelton, et al. (1995). "Flocculation of Polystyrene Latex by Polyacrylamide-Copolyethylene Glycol." Journal of Colloid and Interface Science **175**(1): 166-172.